INJECTION MOLDING OF POLYMERIC MICROFLUIDIC DEVICES

A THESIS

SUBMITTED TO THE DEPARTMENT OF MECHANICAL

ENGINEERING

AND THE GRADUATE SCHOOL OF ENGINEERING AND SCIENCE

OF BILKENT UNIVERSITY

IN PARTIAL FULFILLMENT OF THE REQUIREMENTS

FOR THE DEGREE OF

MASTER OF SCIENCE

By

ARİF KORAY KOSKA

October, 2013

I certify that I have read this thesis and that in my opinion it is fully adequate, in scope and in quality, as a thesis for the degree of Master of Science.

Assist. Prof. Dr. Barbaros ÇETİN(Advisor)

I certify that I have read this thesis and that in my opinion it is fully adequate, in scope and in quality, as a thesis for the degree of Master of Science.

Assist. Prof. Dr. Merve ERDAL

I certify that I have read this thesis and that in my opinion it is fully adequate, in scope and in quality, as a thesis for the degree of Master of Science.

Assist. Prof. Dr. Yiğit KARPAT

Approved for the Graduate School of Engineering and Science:

Prof. Dr. Levent Onural
Director of the Graduate School

ABSTRACT

INJECTION MOLDING OF POLYMERIC MICROFLUIDIC DEVICES

ARİF KORAY KOSKA
M.S. in Mechanical Engineering
Supervisor: Assist. Prof. Dr. Barbaros ÇETİN
October, 2013

Mass-production of microfluidic devices is important for fields in which disposable devices are widely used such as clinical diagnostic and biotechnology. Injection molding is a well-known, promising process for the production of devices on a mass-scale at low-cost. The major objective of this study is to develop a technique for repeatable, productive and accurate fabrication of integrated microfluidic devices on a mass production scale. To achieve this, injection molding process is adapted for the fabrication of a microfluidic device with a single microchannel. During the design procedure, numerical experimentation was performed using Moldflow® simulation tool. To increase the product quality, high-precision mechanical machining is utilized for the manufacturing of the mold of the microfluidic device. A conventional injection molding machine is implemented for the injection molding process of the microfluidic device. Injection molding is performed at different mold temperatures. The warpage of the injected pieces is characterized by measuring the part deformation. The effect of the mold temperature on the quality of the final device is assessed in terms of part deformation and the bonding quality. From the experimental results, one-to-one correspondence between the warpage and the bonding quality of the molded pieces is observed. As the warpage of the pieces decresases, the bonding quality increases. A maximum point for the breaking pressure of the bonding and the minimum point for the warpage was found at the same mold temperature. This mold temperature was named as the optimum temperature for designed microfluidic device. The experimental results are also used to discuss the assessment of the simulation results. It was observed that although Moldflow® can predict many aspects of the process, all the physics of the injection molding process cannot be covered.

Keywords: Polymeric disposable devices, microfluidics, injection molding, warpage characterization, direct bonding.

ÖZET

POLİMER TABANLİ MİKRO-AKIŞKANLAR-DİNAMİĞİ CİHAZLARININ ENJEKSİYON KALIPLAMASI

ARİF KORAY KOSKA
Makina Mühendisliği, Yüksek Lisans
Tez Yöneticisi: Yrd. Doç. Dr. Barbaros ÇETİN
Ekim, 2013

Mikro-akışkanlar-dinamiği cihazlarının seri üretimi, kullan-at tip cihazların yaygın olarak kullanıldığı klinik teşhis ve biyoteknoloji alanları için büyük bir öneme sahiptir. Enjeksiyon kalıplama yöntemi iyi bilinen ve düşük maliyetli seri üretim için uygun bir yöntemdir. Bu çalışmanın amacı bütünleşik mikro-akışkanlar-dinamiği cihazlarının tekrarlanabilir, verimli ve hassas bir şekilde seri üretimini yapabilecek bir metot geliştirmektir. Bu amaçla, enjeksiyon kalıplama yöntemi mikro-akışkanlar-dinamiği cihazlarının seri üretimi için uyarlanmıştır. Tasarım sürecinde, sayısal deneyler Moldflow® simulasyon programı kullanılarak yapılmıştır. Ürün kalitesini arttırmak için, tasarlanan kalıp yüksek hassasiyetli mekanik işleme yöntemiyle üretilmiştir. Klasik enjeksiyon makinası mikro-akışkanlar-dinamii cihazının üretilmesi için adapte edilmiştir. Enjeksiyon kalıplaması farklı kalıp sıcaklıklarında uygulanmıştır. Enjekte edilen parçaların burkulma karakterizasyonu, parça deformasyonu incelenilerek yapılmıştır. Kalıp sıcaklığının ürün kalitesine etkisi deformasyon ve bağlanma kalitesi açılarından incelenmiştir. Deney sonuçları ışığında burkulma ve bağlanma kalitesinin bire-bir ilişkili olduğu gözlemlenmiştir. Parça burkulması azalırken, fiziksel bağlanma kuvvetinde artış görülmüştür. En düşük burkulmanın gözlemlendiği kalıp sıcaklığında üretilen parçaların, basınç dayanımlarının diğerlerine göre en yüksek olduğu görülmüştür. Bu kalıp sıcaklığı, tasarlanan mikro-akışkanlar-dinamiği cihazı için en uygun sıcaklıktır. Deney sonuçları, simulasyon sonuçlarıyla karşılaştırılmıştır. Bunların ışığında, Moldflow® simulasyon programının enjeksiyon kalıbı tasarımı için bir çok açıdan iyi olmasına rağmen, enjeksiyon kalıplama sürecinin tüm fiziğini kapsayamadığı gözlemlenmiştir.

Anahtar sözcükler: Polimer tabanlı kullan-at cihazlar, mikro-akışkanlar-dinamiği, enjeksiyon kalıplama burkulma karakterizasyonu, fiziksel bağlanma.

Acknowledgement

I would like to express my gratitude to my family for their endless patience and support during my long education life. They never gave up believing in me. I would not have been able to complete this work without them.

Special thanks go to Dr. Barbaros Çetin for his professional guidance, encouragement and trust which has been going on since my undergraduate years. He is the best instructor in my life.

I would like to thank Dr. Yiğit Karpat and Dr. Merve Erdal for their guidance and help.

I would like to thank Dr. Sinan Filiz for his trust and believing to me while getting acceptance from Bilkent University.

I would also thank all my friends at Bilkent University, especially Ateş Erdoğan, Mustafa Kara, Mehmet Dogan Aşık and Şaban Uzgör for their friendship and assistance.

Last, but not least, I want to thank Mustafa Kılıç and Şakir Baytaroğlu for their motivation and their help.

Contents

List of Figures

List of Tables

Chapter 1

Introduction

1.1 Injection Molding

Injection molding is one of the manufacturing processes. Melted material is injected into a mold to get desired shape. Materials used are generally plastics (thermoplastics, thermosettings and elastomers), ceramics and metals. During the process, the selected injection material is supplied into a heated barrel, mixed, and forced into a mold cavity where it cools and solidifies correspond to the shape of the cavity [4]. This method is probably one of the most well-known technologies [5]. Injection molding has been used over the century. Its history started in late 1800's. John Wesley Hyatt and his brother Isaiah patented the primary injection molding machine in 1872 [6]. The machine was the simplest and most primitive one. This machine produced simple products like collar stays, buttons, and hair combs [7].

Injection molding is an ideal manufacturing process to fabricate parts on mass scale; hence, it is widely used in many areas such as aerospace, automotive, medical, toys and optics [8]. Nearly, all of the plastic products which can be seen in our daily life are being produced by injection molding, such as mobile phone housings, automobile bumpers, television cabinets, compact discs, lunch boxes, mouse housing, pencil, etc [9]. Some of the application fields and products are

listed in Table 1.1 [10]. This process is also becoming common to produce devices used in less common applications [11].

Table 1.1: Application fields of injection molding

Main Industries	**Components Example**
Automotive	Connectors
Computer	Printer ink heads
Telecommunication	Fiber optics connectors
Sensors	Airbag sensors
Micromechanics	Rotators
Optics	Lenses, displays
Watch Industry	Cog-wheel
GF-Transmission	Connectors
Medical	Hearing aid, implants

There are certain advantages associated with the injection molding process which can be summarized as [2, 12]:

- Injection molding is one of the best technique that can offer mass-production capabilities with relatively low costs.
- Injection molding is a well-known and well-developed technology.
- Once a mold has been manufactured, several thousand parts can be molded with little or no extra effort.
- The cost of raw material is usually negligibly low, since only a small amount of material is required for micro-featured designs.
- Have a good dimensional tolerance and require almost no finishing operations on the final product.
- It is useful for fibers, polymers, ceramics and metals.

- Capabilities of very small features (depending on the quality if the manufacturing of the mold).

On the other hand, it is not a preferred method of manufacturing for short production runs or rapid prototyping. This is mainly due to the cost of tooling and the cost of operation.

A polymer injection molding process conventionally composed of four steps: **(i)** filling of the melted polymer into the mold, **(ii)** packing of more melted polymer into the mold under high pressure to compensate for shrinkage of the material as it cools, **(iii)** cooling of the melted polymer until it solidifies and becomes sufficiently solid, **(iv)** demolding of the solidified part from the mold [11].

There are also challenges associated with injection molding process. These challenges can be grouped into three main titles:

(i) The nature of injection molding (in particular the basic physics of the process): First challenge comes from the nature of the injection molding process, since the injection molding process involves several heat transfer mechanisms, is transient in nature, and involves a phase change and time varying boundary conditions at the frozen layer during filling, packing and cooling. While these challenges are substantive, the process become more complicated by material properties and the geometry of the product [11].

(ii) Material properties: In the injection molding, materials widely used are polymers which can be classified as semi-crystalline or amorphous. Both have complex thermo-rheological behavior which could be seen on the molding process. Thermal properties of thermoplastics are temperature dependent and may also depend on the state of the stress [13]. For semi-crystalline materials, properties also depend on the flow history and rate of temperature change [11]. Especially for the simulation of the injection molding process, an additional complexity comes from the need for an equation of state to calculate the density variation as a function of temperature and pressure [11].

(iii) Geometric complexity of the mold: Injection molded parts are typically thin-walled structures and may have extremely complex structures. The combination of thin walls and high injection speeds causes significant flow and shear rates ans coupling of these with the material's complex viscosity characteristics causes also large variations in material viscosity and in fill patterns [11]. The mold has two tasks in injection molding. The first task is to give the desired shape and the second one is to remove the heat from the mold [11]. An injection molding is a difficult mechanism with provision for moving melted material and ejection systems [11]. This complexity influences the positioning of cooling channels which can affect the variations in mold temperature and these variations changes the material viscosity and the final flow characteristics of the melted material [11].

1.2 Micro-Injection Molding

Micro-injection molding is the process of transferring the micrometer or even sub-micrometer features of molds to a product [1]. During the micro-injection molding, a thermoplastic or thermosetting material which is generally in the form of small particles, is fed from a hopper into a heated barrel where it becomes melted. Then, the melted material is forced into a micro- or nano-featured mold cavity where it is faced to a holding pressure for some time to overcome for the material shrinkage [1]. The melted material solidifies when the mold temperature is decreased below the glass-transition temperature (T_g) of the material. After a sufficient time, the material gets the mold shape and ejected, and the cycle (takes between few seconds to few minutes) is repeated [1].

Micro-injection molding is a very unique injection molding process which requires a specialized molding machine capable of delivering melted material with high injection speed, high injection pressure, precise shot control, uniform melt temperature and ultra-fine resolution using servo-electric drives and sophisticated controls [10]. Micro-injection molding is one of the five micro-molding methods which are the reaction injection molding, hot embossing, injection compression

molding, thermoforming and micro-injection molding [14].

The first development phase of micro-injection technology was between 1985 and 1995 [15]. During that period, injection molding technology was used for macro parts with micro-structured details or features, since there did not exist an appropriate micro-injection molding machine. There were only modified commercial macro-injection molding machines, which were hydraulically driven and with a clamping force of usually 25 to 50 tons [12]. These machines were used as the subtle way of replicating micro-structured mold inserts with high aspect ratios by injection molding [12]. Between 1995 and 2000, the second development phase occurred with the collaboration between mechanical engineering companies and the research institutes. Special micro-injection units or even completely new machines for the manufacturing of real micro-parts were developed in that period [12]. The goal was to decrease the minimal amount of injected material, which is necessary to ensure a stable injection molding (which improves the process repeatability) and increase the replication skills of very small features which was down to 20 μm [12]. After 2000, many leading companies have developed micro-injection molding machines some of which had even special features, like robotic arms for handling etc. The minimum shot weight was down to 25 mg, the wall thickness of the micro-injection molded polymeric micro-structures was down to 10 μm, structural details were in the range of 0.2 μm, surface roughness of about Rz < 0.05 μm and aspect ratio were reached to 20 [16].

The first paper on micro-molding of thermoplastic polymers was printed by RCA Laboratories at Princeton, NJ, USA in 1970 [17]. In this paper, researchers' aim was to find a low-cost reproduction technique of hologram motion pictures for television playback [18]. The mold was fabricated by the electroplating of nickel into photo resist patterns was run through heated rollers together with a vinyl tape and the micro-structure shifted into the vinyl [17]. This work was followed by a study from Zurich, Switzerland [19] in 1976; diffraction gratings for color filtering were fabricated by hot embossing and the aspect ratio (depth/width) of the micro-structure reached up to 5.7 [14]. Micro-molding technique was also used to produce optical waveguides in 1972 [20]. A simple groove was opened onto PMMA with a glass fiber by using hot embossing method. Then the groove was filled

with poly cyclohexyl methacrylate (PCHMA) which had a higher optical index. In the mid-1980s, LIGA was developed to manufacture micro-structures [21, 22] in Germany. In a following study, the product was fabricated by using reaction injection molding [23]. In the later studies, the reaction injection molding modified to an injection molding, since it is much easier process, which can be made with a shorter cycle time [24, 25]. During the first years of the fabrication of the products with micro-molding technique demonstrated that high aspect ratios, steep side walls, and stepped profiles can be achieved and various materials can be used [24, 25]. Due to these developments in micro-molding, it turned out to be the most important production step of LIGA, not only for academic research, but also for the industrial applications. This low-cost method brought an economic benefit to LIGA [14]. Meanwhile, the development of new micro-molding method based on hot embossing had been introduced at Karlsruhe in 1993 [26]. The goal of this research was to develop a way to manufacture a molded LIGA microstructure on top of electronic circuits, such as the fabrication of an acceleration sensor directly on top of an amplifying circuit on a silicon substrate [27]. After becoming more eligible for molding micro-structures with aspect ratios as high as 10 and together with the development of low mechanical stress in the products, hot embossing process was also used to fabricate other devices as well such as micro-valve etc. [28, 29]. In 1993, a group of scientists from Zurich, Switzerland reported that the hot embossing of integrated optical micro-structures [30, 31]. Two years later, a group from Mainz, Germany, published their work which was the fabrication of some optical components by hot embossing [32]. Later, other researches on micro-molding of thermoplastic polymers followed from Santa Cruz, CA, USA [33], Middleborough, UK [34], Dortmund, Germany [35], Stockholm, Sweden [36], Ann Arbor, MI, USA [37], Hayward, CA, USA [38], Gaithersburg, MD,USA [38], Jena, Germany [39], and Taiwan [40].

Micro-molding was also utilized for the fabrication of micropumps and their components [41]. which are generally used for medical, chemical and environmental technologies [42–47]. The pump was fabricated by using injection molding method and its material was polysulfone (PSU). Firstly, two housing shells were fabricated. Then, they were adhesively bonded to a membrane which was

produced of polyimide patterned by photolithography [14]. The mold was manufactured by conventional milling. The whole manufacturing process of the micropump was called the AMANDA process [48]. Today, the AMANDA process is still in use to manufacture microfluidic devices [14]. Micro-pumps [49, 50], micro-valves [51, 52], and micro-sensors [53] have been produced by the same or similar methods. With the developments in nanotechnology, the manufacturing of the mold inserts with structures even in the nanometer range is possible nowadays [54].

Considering the micro-systems, microfluidics and molding market, there has been a rapid increase in the last decade. In 2003, the market was $50 billion. In 2005, it jumped to $68 billion. When 2010 was reached, it was $200billion all over the world [54]. In terms of total plastic consumption, injection molding is at the second ranking. Resin consumption, for USA injection molders alone, is expected to grow at 3.2 percent per annum for the next few years [55]. On the other hand, microfluidic products' market volume was approximately $600 million in 2006, and for 2012 it was estimated $1.9 billion [56].

Micro-injection molding has been used in many areas for different kind of applications: micro-optical, electronics, such as gratings, waveguides, capacitor housing, ceramic ferrule holder, micro-connectors and lenses [10, 42, 44–47, 57], micro-mechanical applications, such as micro-springs, catch wheel gears and miniaturized switches [10,42,44–46], sensors and actuators, such as sensors of flow-rates [46, 57], medical and surgical, such as blade holder, dental prosthetic [10]. Micro-injection molding is also one of the main manufacturing techniques to produce polymeric microfluidic devices which are mainly used for medical diagnostics, sample absorption, separation, mixing with reagents, analysis and waste absorption [1]. Some DNA analysis systems which are generally produced by glass, are currently being produced by polymers [43, 57]. In the literature, it has been reported that micro-injection molding was used for capillary electrophoresis (CE) platforms [43, 46, 57–59], miniaturized heat-exchangers [42] and nanofilters [43]. There are also some commercial companies which produce microfluidic systems using micro-injection molding like Bartels Microtechnik [60], Thinxxs [61], Micralyne [62] and Microfludic ChipShop [63].

Table 1.2: Comparison between macro and micro-injection molding

Process	**Injection Molding**	**Micro-injection molding**
Machine	Hydraulic and electrical machines	Electrical or electro-pneumatic
	Clamping Force $>$ 15 tons	Clamping Force $<$ 15 tons
Flow simulation	2.5D calculation	3D calculation is required
Mold development	CAD rules for the part geometry	Simulation of the feeding channel
	Injection gate diameter $>$ 1mm	Injection gate diameter $<$ 1mm
Realization	CNC Machining	CNC machining or EDM for base mold
	EDM	LIGA, μEDM, ECM, Laser ablation, DRIE
Plasticization	Screw (>20mm) and thermal heating	Plasticization screw (<20mm) or Plunger
Injection	Shear rates $< 10^4 s^{-1}$	Shear rates $> 10^6 s^{-1}$
Temperature	Manufacturer's recommended	Higher than manufacturer's recommended
		Variotherm process for the mold
Holding	Switchover set as a function of the pressure	Switchover based on the plunger position
		Rapid freezing of the injection gate
Cooling	Generally few tenths of seconds	Instantaneous cooling
Part control	Parts masses and dimensions	Dimensional tolerances, Part functioning

The micro-injection molding is not simply a scaling down of the conventional injection molding process. It needs some important modifications not only in methods but also in practice [3]. To illustrate these modifications, a non-exhaustive list of the differences existing between these two techniques is given in Table 1.2 [3]. As shown in Table 1.2, the scaling down of the products requires a changes of each process parameter such as cooling, holding, temperature etc. Moreover, sometimes the development of specific systems is also needed in the goal of realizing micro-products. The use of finite elements and finite differences approaches in injection molding described as a hybrid approach. Moreover, as the pressure field is 2D and the velocity and temperature field are 3D, this method

of molding simulation is often referred to as 2.5D analysis [11].

Giboz [3] is the first scientist who experimentally showed the differences between the polymer characteristics injected with conventional and micro-injection machines. He showed the changes in polymer structure which is subjected to extreme processing conditions during the micro-injection molding. The results was that it leads to a significant change of the polymer structure, and in particular in the size of the crystalline entities or the degree of crystallinity, because of the high cooling rate and/or the shear imposed to samples [3].

Although it is not possible to simply scale down the proces, it is possible to adapt macro-injection molding machines to manufacture micro-parts. There are several technical changes which are necessary to produce injection machines capable of manufacturing micro-products [1]. These modifications can be listed as follows:

(i) Smaller injection (plastification) unit: Reducing the size of the injection (plastification) unit needs the reduction of the screw size and also mofidifcation in its design parameters, like residence time, length to diameter ratio (L/D ratio), root diameter, and compression ratio [1]. Strength is the one of the critical limitations to screw diameter, since the screw should resist the torque needed to carry the solid material through the transition area [1]. Moreover, the general pellet size imposes limits on the screw flight size. In micro-injection molding machine, general injection unit diameters are 14 and 18 mm with L/D ratios of 15 to 18 [1].

(ii) Lower tonnage: Injection molding of micro-parts needs less projected area, which is the area of the mold surface occupied by the mold cavity [1]. Hence, a clamping unit with lower tonnage was needed [1, 64]. Both mechanical toggle and hydraulic clamp systems are convenient for micro-scale injection molding. The conventional system (classic injection molding machine) is less complex, where as the latter (modified injection molding machine) is more precise for small shot sizes [65].

(iii) Advanced control system: A precise control system is required to meter smaller shot sizes [1]. The accuracy of the control system depends on the control mechanism response time and the resolution of the positional indicator [65]. Moreover, a precise parameter-control is required for better reproducibility [43], especially in the changeover from injection pressure to holding pressure [46].

(iv) Variotherm process: The well-known classic or macro scale injection molding can be modified to the micro-scale by also employing a *Variotherm Process* [14,66]. In this process, the mold is heated up to the glass transition temperature (T_g) of the polymer, and when the mold is completely filled, and cooled down rapidly using additional cooling lines inside the mold [1]. This cyclic temperature control system is called variotherm (variothermal) and process is called as *Variotherm Process* [43, 57].

(v) Air evacuation: In order to prevent air bubbles in the product, the mold cavity has to be evacuated using an external evacuation system [45, 57].

Besides the advantages of the injection molding, micro-injection molding introduces some more advantages such as capabilities of very small features (down to 20μm), minimum shot weights down to 5 mg [12]. However, these advantages comes with a price. Micro-injection molding machine cost is relatively high, changing the polymer used in the machine is challenging due to the compact nature of the micro-injection molding machines machines.

1.3 Objectives and Motivation

Micro- and nano-scale fabrication of disposable medical devices is a popular topic not only for research opportunities but also for commercial opportunities. Injection molding of thermoplastic polymers is a developing process with great potential for producing mass amount of micro-scale devices at low-cost [1]. This kind of repeatable, productive, mass-scale production of microfluidic devices is important especially for fields in which disposable devices are widely used such

as drug delivery, clinical diagnostic and biotechnology. The major objective of this study is to develop a technique for repeatable, productive and accurate fabrication of integrated microfluidic devices on a mass production scale. To achieve this, injection molding process is adapted for the fabrication of a microfluidic device with micro-features (e.g. a microfluidic device with a single microchannel). For the design of the mold, simulations are performed using commercial software Moldflow®. A conventional injection molding machine is utilized for the injection molding process; however, to increase the product quality, the mold of the product is manufactured by using high-precision mechanical machining. Injection molding is performed at different mold temperatures, and the effect of the mold temperature on the quality of the final device is assessed in terms of part deformation (which is related to the warpage of the products) and the bonding quality. The experimental results are used to discuss the assessment of the simulations. To the best knowledge of the authors, this study is one of the pioneers in terms of the characterization of the warpage of a microfluidic device (i.e. product with micro-feature). Moreover, this is the first study regarding the application of injection molding for microfluidic devices in Turkey.

1.4 Outline of the Thesis

In **Chapter 1**, the literature survey on injection molding and micro-injection molding is presented. Advantages, disadvantages, challenges, applications, market of injection molding and micro-injection molding are discussed. In **Chapter 2**, the design procedure of the mold and the material selection are discussed. The CAD design of the mold was performed using SolidWorks. In order to check the mold design and to find the best injection conditions in terms of the mold temperature, simulations were performed for different mold temperatures using Moldflow®. The simulations are presented in **Chapter 3**. After the confirmation of the mold design by simulation results, the mold was manufactured. The manufacturing process is discussed in **Chapter 4**. The mold was fabricated by using high-precision mechanical machining and G-codes were generated by using SolidCAM. The injection was performed at different mold temperatures. After the

injection molding experiments, in order to transform injected microchannels to a real microfluidic device, bonding was performed. Direct and adhesive bonding methods were used. The warpage characterization of the injected microchannels were performed and the results are compared with the simulation results. The results are presented and discussed in **Chapter 5**. Finally, the major findings and the future research directions are summarized in **Chapter 6**.

Chapter 2

Mold Design and Material Selection

2.1 Mold Design

There are some critical design rules which should be followed while designing a mold. Firstly, all of the sharp corners must be refrained in the design, since they result in stress peaks in the product, which may cause cracks [14]. Most of the problems in injection molding are not caused by the filling process of the mold, they are caused by demolding process [14]. If the mold is not designed properly or if inappropriate molding variables are selected, especially micro-structures may be cracked, torn apart, deformed, or destroyed during demolding process [14]. Demolding process can also cause wear of mold inserts and may even destroy delicate parts of the mold insert after a single injection [14]. It is possible to eject micro-structures with vertical side walls by giving an inclination or draft angle of just 2°–5°, it significantly reduces the demolding forces [14]. This issue is vital and even more important than the roughness of the side walls for the products with micro-features [14]. One of the important factors in demolding is the shrinkage of the material, which occurs during the cooling down of the

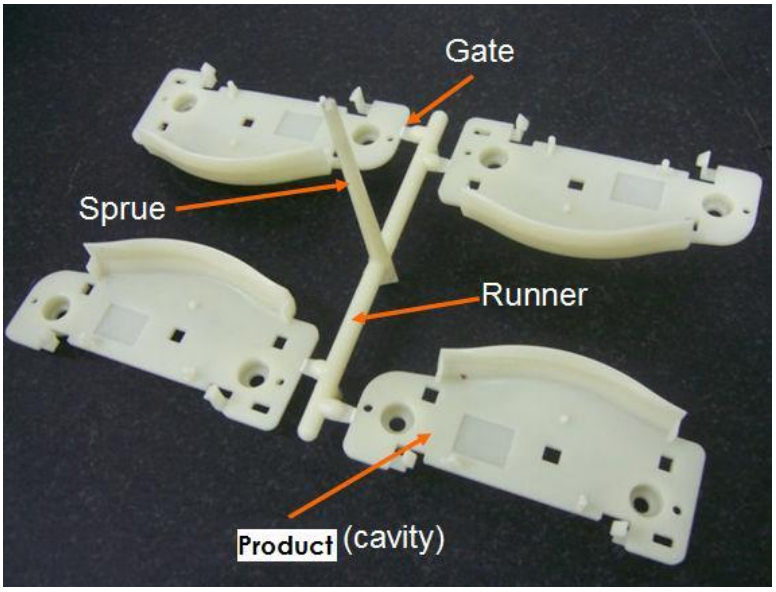

Figure 2.1: A representative photograph to show sprue, gate and runner.

material between the filling and demolding processes [67]. As a result, the demolding forces become functions of the orientation of micro-structures relative to the direction of shrinkage and the location of critical micro-structures relative to the center of shrinkage [14]. Delicate micro-structures, like pins with high aspect ratios, can be saved against shear forces resulting from the shrinkage by the inclusion of neighboring auxiliary structures which are stable enough to resist these shear forces [14].

For a proper or complete design of a mold, the major components of the mold such as sprue, runner, gate, pushing pins and air vents needs to be designed properly. A representative photograph to show sprue, gate and runner can be seen in Figure 2.1. The significance and some design criteria of these major components can be summarized as follows:

(i) Sprue: A sprue is the passage through which the molten material is introduced before getting into the runner. During the injection molding, the material in the sprue solidifies and it needs to be removed from the mold. For an easy removal; it should be in conical shape: 3°–5° taper is given on the inner diameter of the sprue bush [68]. This is very crucial for repeated

cycles. Moreover, the inner surface of the sprue needs to be very smooth to avoid the resistance during the removal of the solidified material. Due to this reason, surface finishing operations may be needed after manufacturing the sprue.

(ii) Runner: Runner is a channel through which the resin or melted material enters the gates of the mold cavity and it connects the gate and the sprue [69]. To make the flow of the melted material smoother, the runner should be as thick as possible, short, well-placed, and each corner should be rounded for a smaller flow resistance in the runner [68]. When the melted material flows through the runner, the resin close to the mold will solidify by decreased temperature. This solidified resin works as a heat insulator; hence, a circular shape is the ideal for runner [68].

(iii) Gate: Gate is the entry-way for the resin into the mold cavity [69]. Generally, for symmetric and thin-walled structures, it is better for the the gate to be located at the center of the edge, in rectangular shape, have a thickness which is one-third of the thickness of the runner, and have a width which is more than the width of the runner. The gate design critical for smooth and easy filling [68].

(iv) Pushing (ejector) pins: Pushing pins help open the mold and remove the products from the mold easily. The important design consideration is that the outer pins (which help open the mold) should be in negative tolerances and the inner pins (which help eject part from the mold cavity) must be in positive tolerances in terms of length. Otherwise, the mold is not closed properly and it would be hard to remove products from the mold. Moreover, in terms of diameter, inner pins need to be tight enough to prevent the leakage of the injected material.

(v) Air vents: Trapped air in the mold cavity can exit through air vents embedded in the mold. If the trapped air is not permitted to exit or the venting is not enough, the air is compressed by the pressure of the entering material and squeezed into the corners of the cavity, which prevents proper filling of the material and may also cause defects like bubbles in the final

product [8]. The trapped air may even become so compressed that it may ignite and burns the surrounding material [8]. Air vents generally need to be machined at the opposite side of the gate and located at the corners which make filling easier and smoother [68].

(vi) Depth of the mold cavity: Depth of the mold cavity is another important design consideration. As the depth of the mold cavity increases, so do the the cooling time and temperature variation which may lead to warpage and surge.

(vii) Additional cavity: Generally, melted material which was injected at the begining of the cycle, may include some burned or different materials from the previous injection cycle. Avoiding these contaminations is important especially when the mass-scale production with very high number repeated cycles is considered. Therefore, in order to keep these contaminations away from the mold cavity, additional cavity needs to be machined in the mold.

Considering the aforementioned design criteria, the mold was designed for the injection molding of a microfluidic device. The rendered image of the CAD drawing of the mold can be seen in Figure 2.2 (the technical drawing of the mold can be found in the Appendix). The mold has two different single microchannel structures as seen in Figure 2.2 (one of the microchannel structure is highlighted by green). Lengths of microchannels are 10 mm and 20 mm, their width and depth are 200 μm. This kind of microfluidic device is suitable for high performance liquid chromatography (HPLC) applications. The mold consists of the top and the bottom part of the microfluidic device. The inlet and outlet reservoir openings (2 mm in diameter) are included at the bottom part (highlighted by black in Figure 2.2), and the microchannel is included at the top part. For the ease of the demolding process, 5° draft angle was introduced at the side walls of the microchannels and the mold cavity. To avoid turnabout (reverse flow of the melted material which causes additional flow resistance) of the resin, v-shaped runners with guidance way are included in the design (guidance way is also used to prevent melted material to enter the mold cavity with an angle which may prevent smooth filling of the mold cavity and cause cooling differences). As mentioned

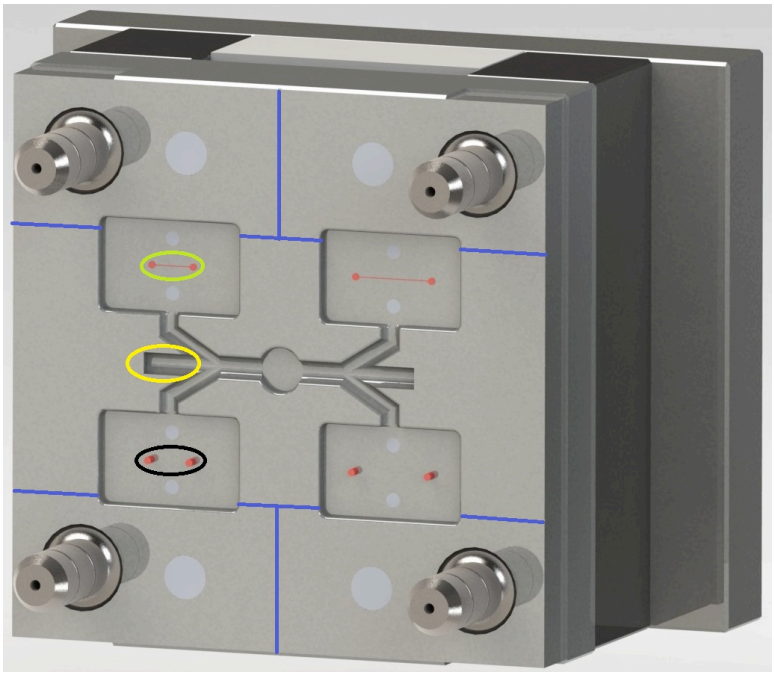

Figure 2.2: Rendered image of the CAD drawing of the mold

in (vii), additional cavities are included (highlighted by yellow in Figure 2.2) in the mold which ensures the use of the mold on a mass-scale without any contamination problem. To ensure easy and smooth filling, air vents (shown by blue lines in Figure 2.2) are also introduced in the design. For the ease of demolding, houses for pushing pins are added to the mold (can be seen as gray circles in Figure 2.2). The depth of the mold cavity is chosen as 3 mm for ease of handling of the product.

2.2 Material Selection

Glass, silicon and polymers have been generally used for the fabrication of the products with micro-features. However, polymeric materials have some certain advantages over glass and silicon as:

(i) Polymers are relatively low in cost, especially useful for mass production disposable devices [70, 71].

Table 2.1: Polymers commonly used for injection molding [1]

Polymers	**Abbr.**	**Aspect Ratio**	**Thickness** [μm]	**Application**
Polymethyl methacrylate	PMMA	20	20	Optical fibre connector
Polycarbonate	PC	7	350	Cell Container
		4–8	0.2–0.5	Optical element
Polyamide	PA	10	50	Micro gear wheels
Polyoxy-methyleme	POM	5	50	Filter with defined pore diameters
		10	80	Micro-rods
Polysulfone	PSU	5	270	Microfluidic device housings
Polyether-etherketone	PEEK	5	270	Housing for micro-pumps
Liquid crystal polymers	LCP	5	270	Microelectronic devices
Polyethylene (High density)	HDPE	8	125	High aspect ratio squares
		10	225	Micro-wells
Cyclic Olefin Copolymer	COC	0.02–2	0.1–0.9	Microfluidic patterns

(ii) Material costs are not greatly affected by the complexity of the design, as design complexity mostly impacts on mold manufacturing cost rather than on the molding process itself [14, 43, 72, 73].

(iii) Polymers have a broad range of characteristic material properties, like different mechanical strength, optical transparency, chemical stability and bio-compatibility; hence, using polymer helps obtain needed properties easily for the processing and the application [14, 43, 70, 73, 74].

Selection of the suitable polymer for the injection molding of microfluidic components is one of the most difficult tasks in the design process for microfluidic applications, since some considerations have to be taken into account such as the effect of polymer on achievable product tolerances and satisfying the material

Table 2.2: Typical characteristics of different polymers for injection molding [2]

Polymers	**PMMA**	**PS**	**PA**	**COC**	**PP**
Heat Resistance [°C]	105	140	100	130	110
Density [kg/m^3]	1190	1200	1050	1020	900
Refractive Index	1.42	1.58	1.59	1.53	Opaque
Resistant to:					
Aqueous solutions	yes	limited	yes	yes	yes
Concentrated acids	no	no	yes	yes	yes
Polar hydrocabons	no	limited	limited	yes	yes
Hydrocabons	yes	yes	no	no	no
Suitable for micro-molding	moderate	good	good	good	moderate
Regressors Permeability coefficients [$\times 10^{-17}$m^2/s–Pa]					
He	5.2	7.5	–	–	–
O_2	0.12	1.1	–	–	–
H_2O	480–1900	720–1050	–	–	–
Hot-embossing parameters:					
Embossing temp. [°C]	120-130	160-175	–	–	–
Deembossing temp. [°C]	95	135	–	–	–
Embossing pressure [bars]	25–37	25–37	–	–	–
Hold time [s]	30–60	30–60	–	–	–

property requirements [1]. Some important properties of different polymers are tabulated in Tables 2.1 and 2.2 (the data are adapted from [1]).

For microfluidic applications, it is important that the device material is chemically inert (to avoid any interaction with the chemicals within a buffer solution), biocompatible (to avoid any interaction with the bioparticles), transparent (for visual access during the biological process/experiment) and cheap (to allow disposable devices). Considering all these aspects, Evonik plexiglas 6N (PMMA - Acrylics) is preferred in this study (data sheet of Evonik plexiglas 6N can be found in the Appendix).

Chapter 3

Modeling and Simulation

Injection molding is inherently a complex process due to its physics. During the process, two phase change processes occur and melted material shows a non-Newtonian behavior [11]. Therefore, problems experienced during the manufacturing may not be fixed easily by just varying the process conditions unlike the other manufacturing processes [11]. Although the scope is to adjust process conditions to solve one issue, often the change introduces another issue. For instance, increasing the melt temperature which results in decrease in the viscosity of the melt may overcome the filling problem of the mold. However, the increase in the melt temperature may also cause gassing or degradation of the material which may result in unsightly marks on the product [11]. The filing problem may also be fixed by increasing the number of gates or using a different machine which has a bigger reservoir/plunger [11]. Both of these solutions are economically unfavorable: the former which involves significant retooling is time consuming. The latter one needs the replacement of the original machine with a suitable one which erodes the profit margins. Alternatively, simulations can be performed in a relatively cost-efficient manner in the prestages to evaluate the different design options for the product, material and mold [11]. Moreover, some issues can also be addressed before hand by using simulations.

Softwares for the simulation of the molding tool and/or the mold filling process itself can provide useful, but not wholly sufficient assistance for the optimization

of micro-injection molding [16]. It is clear that the processing has a strong affect on the properties of the manufactured part; hence, the part quality is directly related to the processing conditions. In the process, the relationship between the process variables and the product quality is extremely complex; therefore, it is very difficult to gain an understanding of the relationship between the processing and the product quality by experience alone [11]. Moreover, rely on experience may also result in costly and time consuming process [11]. Due to these reasons, simulation tools has been developed for injection molding applications to gain an understanding about the relationship between the processing and the product quality. Due to this need, computer aided engineering has been implemented successfully for injection molding than the other areas of polymer processing [11].

During the injection molding processes (filling, packing and cooling), the melted material shows a complicated thermomechanical history which causes changing in local specific volume [11, 75]. When the melted material is within the mold, it is constrained within the plane of the product and stresses develop in the product during plastification [75]. After ejection, the relaxation of these stresses results in the instantaneous shrinkage which is usually anisotropic and non-uniform throughout the product and extra shrinkage can be seen also during the cooling following ejection [11, 75]. The anisotropic (non-uniform) shrinkage behavior results in some degree of warpage [11]. Different analyses are possible by using simulation tools:

Filling and packing analyses: Filling stage of the injection molding process is most thoroughly studied [11]. The basic principle is to predict pressure and temperature distributions within the mold cavity and the advancement of the melt front [11]. Early work on filling analysis used the finite difference method or analytical solutions in simple geometries, the seminal paper of Hieber and Shen [76] provided a breakthrough [11]. They introduced a hybrid analysis technique for the filling phase where temperature and pressure equations were solved using finite differences and finite elements, respectively [11]. Often referred as 2.5D analysis, this method remained the cornerstone of commercial simulation tools until the mid-1990's when 3D analysis appeared and in the remainder of this work, it was extended for the packing phase [11].

Mold cooling analysis: There are channels in which coolant circulates to extract heat from the mold. The location of the cooling channels related to the product geometry, cavity configuration and the location of the ejection mechanisms and moving components of the mold [11]. Generally, it is not possible to locate them precisely, so the temperature variation occurs both over the mold surface and between the mold halves [11]. It is widespread to simply assume a fixed mold temperature for the simulation of the filling and cooling stages, a better result may be reached by performing a mold cooling analysis, which requires a 3D analysis of heat transfer throughout the mold [11]. Generally, the outputs of cooling analysis are the mold surface temperatures and heat flux (averaged over the injection cycle).

Warpage analysis: One of the great problems in injection molding is the warpage of the product and in order to understand the development of the warpage simulations, it is important to know that the warpage results from inhomogeneous polymer shrinkage [11]. All polymers shrink on the cooling phase which results in the deformation of the product due to the variation in this phase. The problem can be splited into two parts - prediction of the isotropic shrinkage and prediction of anisotropic effects [11]. The former is influenced mostly by the pressure and temperature history of the product and consequently, it can be said that the packing phase is important for the warpage analysis [11]. Development of the anisotropic shrinkage effects is depend on the structure development of the melted material during the solidification. For an amorphous polymer, the molecular orientation is critical and the problem is more difficult for semi-crystalline materials [11]. Then, the warpage simulation rests on the capability to model the filling, packing and cooling phases of the molding process [11].

There are commercial software are available for mold simulation such as Moldex 3D [77], Moldflow® [78], Sigmasoft [79], Epicor® [80], Injecnet [81]. Moldflow® was used as a simulation tool in this study; since, it is proven to be powerful in injection molding field.

Simulation models need many properties or parameters to be defined which are related to the material in use, the parameters of the injection molding machine

(i.e. maximum clamping force, injection pressure etc.), the designed geometry and the process parameters (i.e. mold temperature, cooling time etc.). Simulation model also requires to enable and disable some features to perform different analyses such as filling, packing, cooling, warpage and shrinkage. General properties and parameters required for the simulation model can be listed as:

- Density, viscosity, mechanical properties (elastic modulus, poissons ratio, shear modulus), thermal properties (specific heat, thermal conductivity, heating/cooling rate), melting temperature, $p-v-T$ relation and rheological parameters of the material
- Maximum injection pressure, maximum clamping force, cooling system and coolant of the machine
- Runner, gate, sprue and mold geometry
- Process parameters like filling time, packing time, mold temperature, cooling time, eject temperature, coolant temperature and hold time
- Enable / Disable of

  Viscous heating

  Non-isothermal effects

  Compressible flow

  Gravitational Force

  Flow-induced residual stress in warpage analysis

  In-mold constraint effect

3.1 Moldflow® Simulations

Moldflow® is one of the most powerful tool for macro scale injection molding simulation. In this study, Moldflow® simulation was performed to check the mold design and to find the best injection condition in terms of the mold temperature

before manufacturing of the mold. In order to check the mold design, simulation was performed with advised injection conditions (molding window analysis) by Moldflow®. In order to find the best mold temperature, the simulations were repeated for different mold temperatures (from 35°C to 85°C). However, Moldflow®'s applicability on products with micro-features was questionable prior to this study.

Governing equations, assumptions, approximations and boundary conditions which are used in the Moldflow® simulation are given below. The numerical solution of the equations governing the filling phase was performed in three stages. The calculation of **(i)** the pressure field, **(ii)** the temperature field and **(iii)** the advancement of the flow front. Moldflow® calculates the pressure field using finite element method, temperature field using finite difference method and advancement in flow front, using control volume approach. The motion of the melted material in injection molding is governed by the conservation laws of mass, momentum and energy, respectively [82]. By using conservation of mass and conservation of momentum (linear and angular) equations, the conservation of energy equation is taken the form of [11]:

$$\rho c_p(\frac{\partial T}{\partial t} + \mathbf{v}\cdot\nabla T) = \beta T(\frac{\partial p}{\partial T} + \mathbf{v}\cdot\nabla p) + p\nabla\cdot\mathbf{v} + \underline{\sigma} : \nabla\mathbf{v} + \nabla\cdot(k\nabla T) \quad (3.1)$$

Then, by using material-geometrical assumptions-approximations and mathematical simplifications; the final equation for pressure can be reached as [11]:

$$\nabla\cdot(S\nabla P) = \frac{1}{2}\int_{-H}^{H}\left(\kappa\frac{Dp}{Dt} - \frac{\beta}{\rho cp}\left[\beta T\frac{Dp}{Dt} + \eta\dot{\gamma}^2 + \frac{\partial}{\partial z}\left(k\frac{\partial T}{\partial z}\right)\right]\right)dz \quad (3.2)$$

where;

$$\underline{\sigma} = -p\underline{I} + \underline{\tau} \quad (3.3)$$

$$\kappa = -\frac{1}{v}\left(\frac{\partial v}{\partial p}\right)_T \quad (3.4)$$

$$\beta = \frac{1}{v}\left(\frac{\partial v}{\partial T}\right)_P \quad (3.5)$$

$$\eta = \frac{\eta_o}{1 + \left(\frac{\eta_o \dot{\gamma}}{\tau^*}\right)^{1-n}} \tag{3.6}$$

Table 3.1: List of symbols

Symbol	**Refers to**
S	Fluid conductance
ρ	Density
p	Pressure
$\dot{\gamma}$	Shear rate
H	Half of local thickness
v	Specific volume
k	Thermal conductivity of fluid
c_p	Specific heat
ηo	Viscosity at zero shear
τ^*	Shear stress at transition between Newtonian and power-law behaviour
$\underline{I}$	Identity tensor
$\underline{\tau}$	Viscous or extra stress tensor
$\underline{\sigma}$	Stress in a fluid
κ	Isothermal coefficients of expansion
β	Isothermal coefficients of expansivity
η	Viscosity (cross model)

The description of the symbols used in the equations can be seen in Table 3.1 (the detailed derivation of the governing equations can be found elsewhere [11]).

Moldflow® uses the following assumptions and approximations [11, 83]:

- Fluid is assumed to be in continuum regime. Hence; physical variables such

as density and velocity vary smoothly so that differentiation with respect to both position and time is possible.

- Fluid is compressible.
- The melt temperature and flow rate are assumed constant at the injection point.
- Thin walled assumption; local thickness 2H, is much smaller than a typical length.
- Lubrication approximation; the pressure is assumed constant through the thickness of the part.
- Hele-Shaw approximation; it reduces the conservation equations for mass and force to a single equation for pressure.
- Mold temperature is fixed for filling and cooling analysis.
- Arrhenius or WLF correction, including the effect of temperature on the viscosity.
- Cross model is used for viscosity function.

No slip boundary condition (fluid velocity is zero at the mold wall) was defined as the boundary condition for filling and packing analyses. The mold temperature and the melt temperature of the material are defined as the thermal boundary conditions at the boundaries of the mold cavity. Simulation tools requires the mold geometry as a input parameter (including runner, sprue, gate and cooling channel geometries) and injection material. Moldflow® simulation starts with the creation of the semi-product (inverse or negative of the mold). Semi product (semi-product of the mold can be seen Figure 3.1) was generated directly from the CAD model of the mold by using SolidWorks, and all of the analyses were perfomed on this geometry.

There are two main analysis methods in Moldflow®: dual domain analysis and 3D analysis. Dual domain analysis is appropriate when the part is thin walled

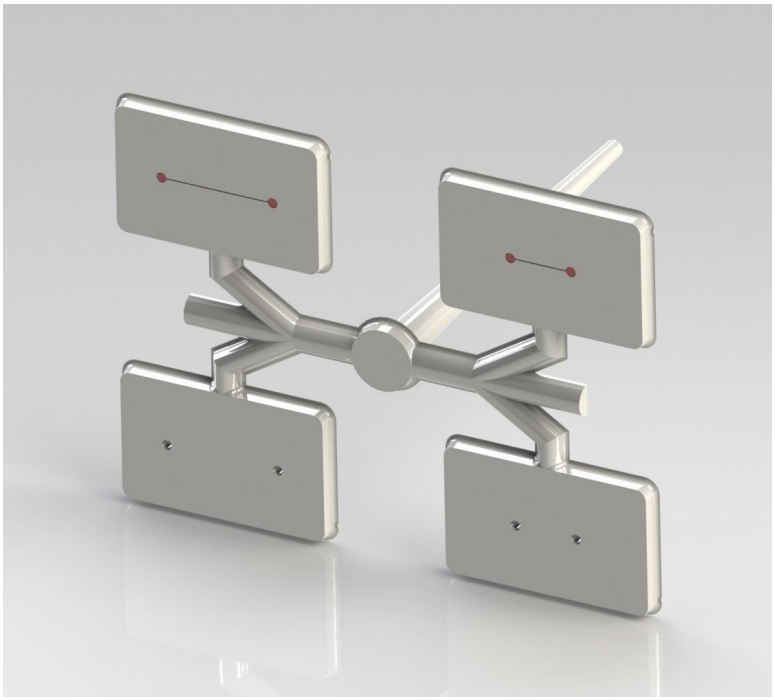

Figure 3.1: Semi-product

with few thick areas. The minimum length and width of any local region need to be greater than four times the local thickness [83]. 3D analysis is appropriate when the product has many thick areas, corners, features or walls. Moreover, 3D analysis is recommended for the products where the length and width of a section is less than four times the local thickness [83]. Since the mold is thin-walled (i.e. height is 3mm), dual domain analysis method was implemented. The input parameter for the simulations are given in Table 3.2. Following analyses were perfomed by using Moldflow®:

(1) Draft angle: Draft angle analysis checks the given draft angles with respect to the demolding direction. As mentioned before, the draft angles are very important for the easy demolding. By the help of this analysis, the direction and magnitude of the draft angle can be checked. The analysis result can be seen in Figure 3.2. In the analysis, parallel area (colored in dark blue) shows the parallelism between the mold cavity floor and the product surface. In other words, this parallel area does not have any effects on the demolding process. Zero draft (colored in red color) shows that there is not any draft angle for the

Table 3.2: Requested parameters by Moldflow®

Parameters	**Value**
Mold temperature	79°C (according to molding window analysis)
Melting temperature	245.3°C (according to molding window analysis)
Injection location	At the Begining of Sprue (according to gate location analysis)
Number of gate	1
Cooling System	None
Max. Inj. Pressure	90 MPa (according to injection machine)
Injection Time	Automatic
Hold Time	Automatic
Injection Material	Plexiglas 6N: Evonik Roehm GmbH

demolding direction. It can be seen that the side walls of the additional cavity's and reservoirs are in red color. However, they do not have much effects on the demolding, since critical areas for the demolding are runner's floor and the side walls of the mold cavity. It can be inferred from the analysis that the draft angle of the critical areas is more than 3° and its direction is suitable for the demolding (3° draft angle is also in the suggested range for the ease of demolding [68]). Therefore, it is not expected to face any problems during the injection.

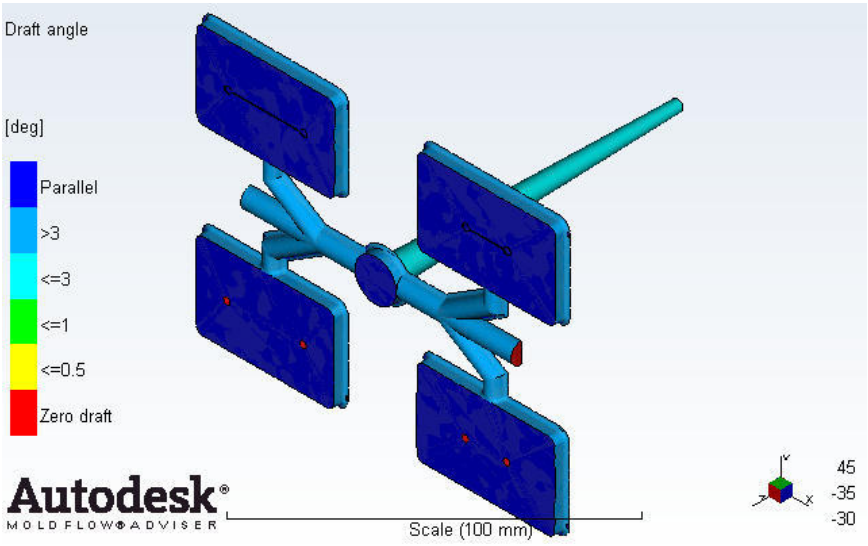

Figure 3.2: Draft angle

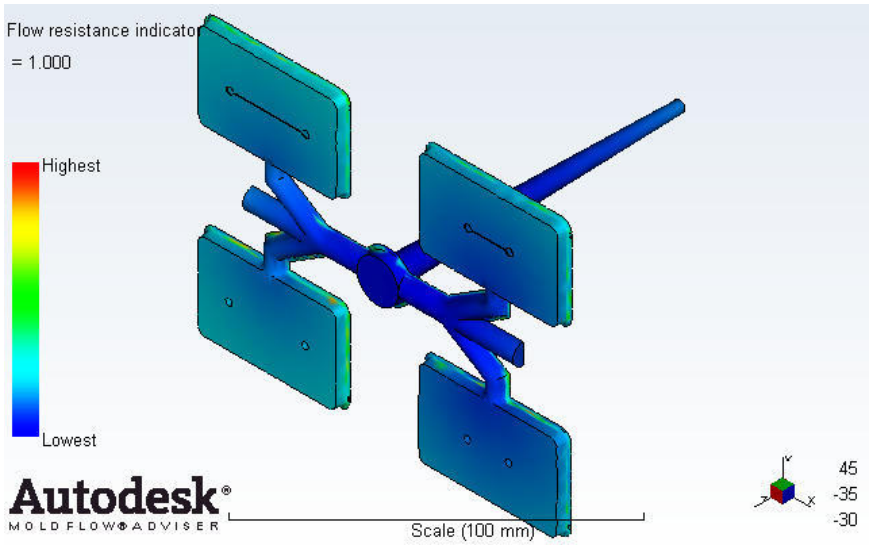

(a)

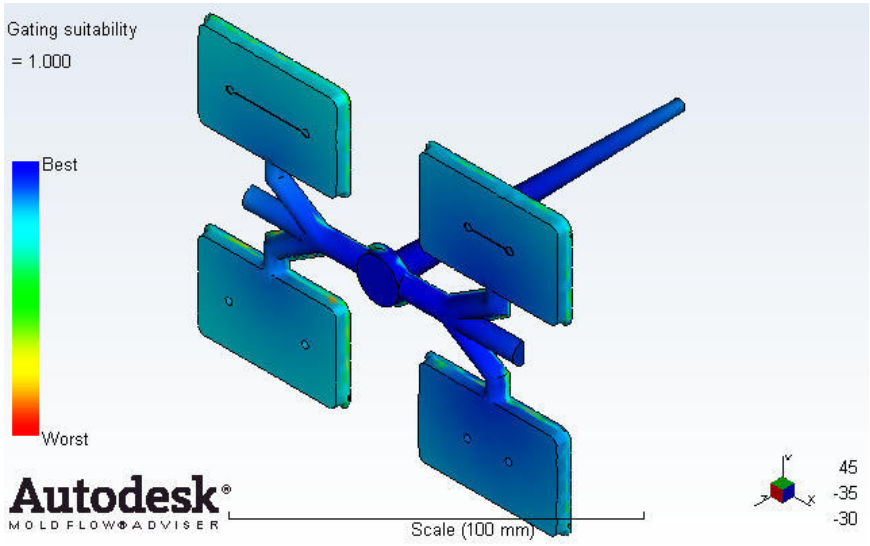

(b)

Figure 3.3: **(a)** Flow resistance **(b)** Gate location

(2) Flow resistance and gate location: The flow resistance analysis shows the resistance at the flow front. The gate region locator algorithm determines and recommends the optimum injection locations based on criteria such as the part geometry, minimum flow resistance, thickness, and molding feasibility [83]. The results for flow resistance and gate location can be seen in Figure 3.3. The most suitable areas for the injection are rated as the best and are colored blue.

The least suitable areas of the model are rated as the worst and colored red. According to the results, general mold design (runner, sprue and mold cavity) is suitable in terms of the flow resistance, since the general flow resistance is low. Moreover, the suggested injection location is located at the entrance of the sprue. All the remaining analyses were performed by setting the injection location at the suggested place.

(3) Molding window: The molding window analysis shows the optimum mold and melt temperatures and the injection time required to produce an acceptable part for a specific material within the constraints of the mold design [83]. Red indicates that there is no feasible molding window, yellow represents a feasible molding window, green represents the preferred molding window. According to Moldflow®, green area ensures the following conditions [83]:

- The part is not a short shot.
- The injection pressure required to fill the part is less than 80% of the maximum machine injection pressure capacity.
- Temperature at the flow front is less than 10°C above the injection (melt) temperature.
- Temperature at the flow front is more than 10°C below the injection (melt) temperature.
- The shear stress is less than the maximum specified for the material in the material database.
- The shear rate is less than the maximum specified value for the material defined in the material database.

The analysis result can be seen in Figure 3.4. According to the molding window analysis, the suggested melt temperature is 245.3°C, the suggested mold tempeature is 79°C, and the injection time is 10 seconds. The reliability of these data will be discussed by comparing with the experimental findings in Chapter 5.

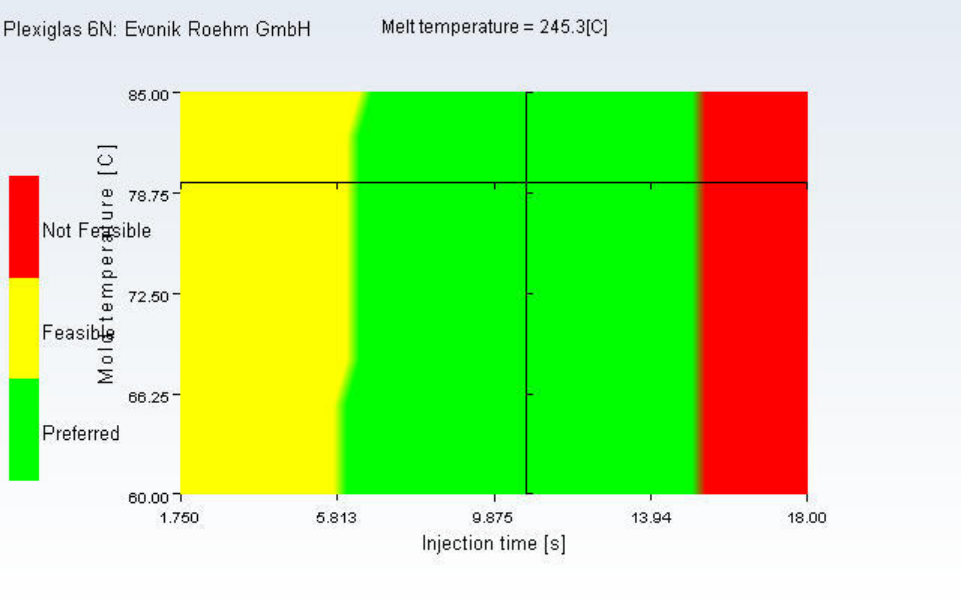

Figure 3.4: Molding window

All the remaining analyses were performed by using the suggested data for the melt temperature, mold temperature and injection time as the input parameters.

(4) Fill time: The fill time analysis indicates the position of the flow front as the cavity is being filled [83]. Regions with the same color refers that they are filled together and the result is dark blue at the start of the injection, and the last areas to fill are in red color [83]. If the part is a short shot, unfilled areas are showed in grey [83]. The contours are evenly spaced and indicate the speed at which the polymer is flowing. Widely-spaced contours refer rapid flow, narrow contours show that the part is filling slowly [83]. The analysis result can be seen in Figure 3.5. Accoding to the result, in order to prevent the short shot, the injection time needs be more than 1.5 second. However, packing time, cooling time and hold time needs also be added up to come up with the time for a complete cycle.

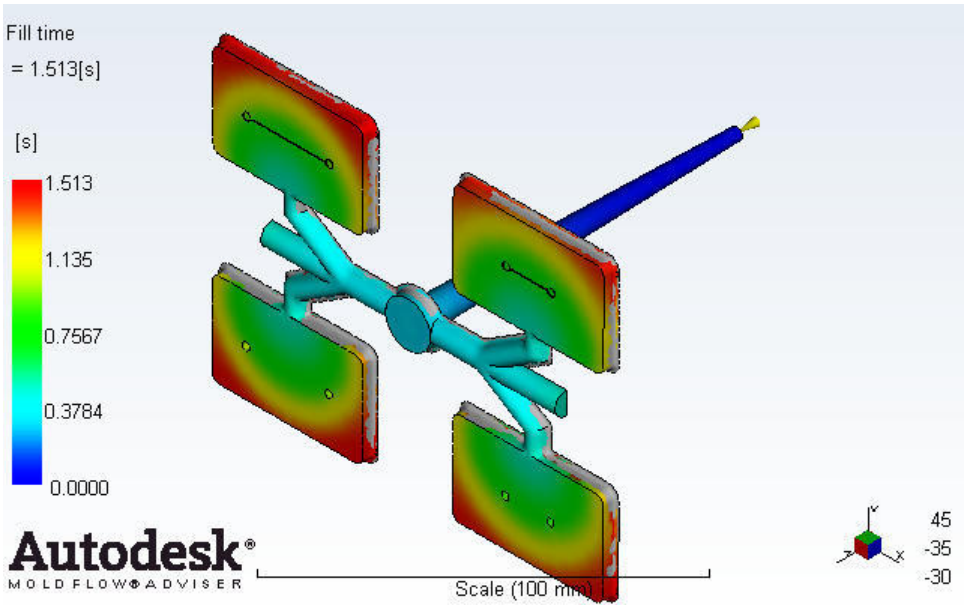

Figure 3.5: Fill time

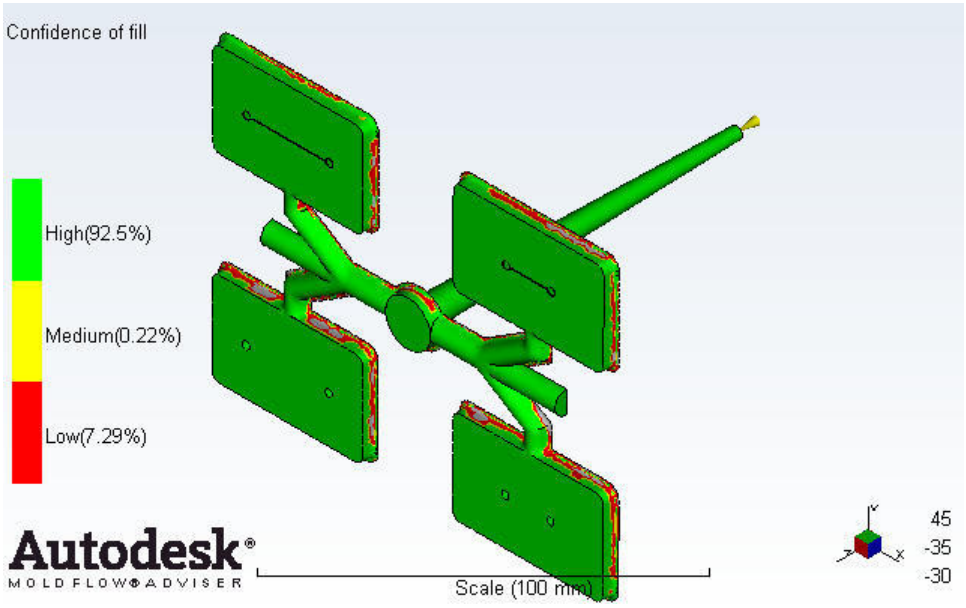

Figure 3.6: Confidence of fill

(5) Confidence of fill: The confidence of fill analysis displays the probability of the plastic filling of a region within the mold cavity under conventional injection molding conditions and the result is obtained as a result of the pressure and

temperature variation [83]. The green color shows the definitely filled areas, the red color indicates the hardly filled areas, and the grey color shows the unfilled areas (short shot). The analysis result can be seen in Figure 3.6. It can be seen that there is no grey area, the mold cavity is expected to be fully filled under the conventional injection conditions. If the cavity did not fill and resulted in a short shot, some modifications would be needed on the design, injection location, choice of plastic, or processing conditions.

(6) Pressure drop: The pressure drop result uses a range of colors to point the region of the highest and lowest pressure drop. This result shows how much pressure is necessary to fill the different areas of the part [83]. The analysis result can be seen in Figure 3.7. It can be seen that pressure drop distribution is symmetric due to the mold design, which leads a smooth filling and symmetric cooling of the mold.

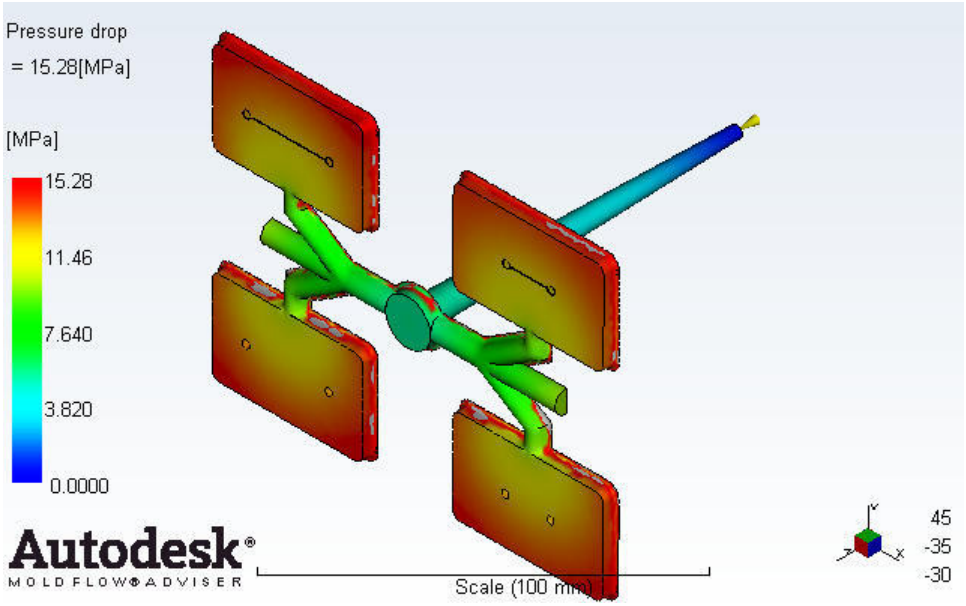

Figure 3.7: Pressure drop

(7) Time to reach the ejection temperature: The time to the reach ejection temperature analysis indicates the time required to reach the ejection temperature, which is measured from the start of filling process [83]. The time to reach the ejection temperature is function of the mold temperature. The analysis result can be seen in Figure 5.2. It can be seen from the analysis that the expected

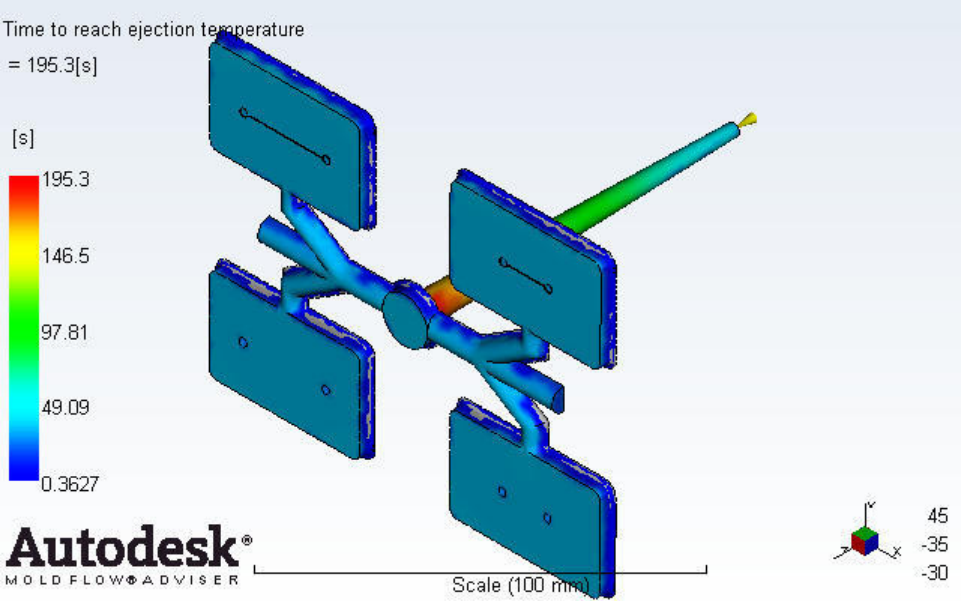

Figure 3.8: Time to reach the ejection temperature

cooling time of the product (i.e. excluding the runner and sprue) is low (blue color in the figure) due to the thin-walled design. It is very important for the determination of the total cycle time. Although the cooling of the sprue side takes too much time (∼195 seconds), it does not affect the cycle time, since the degree of the cooling of the sprue is not critical for the quality of the final product (the critical region is the product itself, and actually the microchannel structure for the microfluidic applications). Moreover, the uniform polymer freeze distribution showed that there is not any cooling difference on the product. This is important to get low warpage for the product.

(8) Weld lines: The weld lines analysis shows the angle of convergence as two flow fronts meet. The presence of weld lines may point a structural weakness and/or a surface blemish [83]. Weld lines can be caused by the melted material flowing around the holes or inserts in the part, multiple injection gates or variable wall thickness where hesitation or "race tracking" may occur [83]. The analysis result can be seen in Figure 3.9. It can be seen from the figure that the expected weld lines are located near the reservoirs. However, these weld lines did not have any effects on the microchannel structure, hence the microfluidic device performance. On the other hand, weld lines are expected have been symmetric

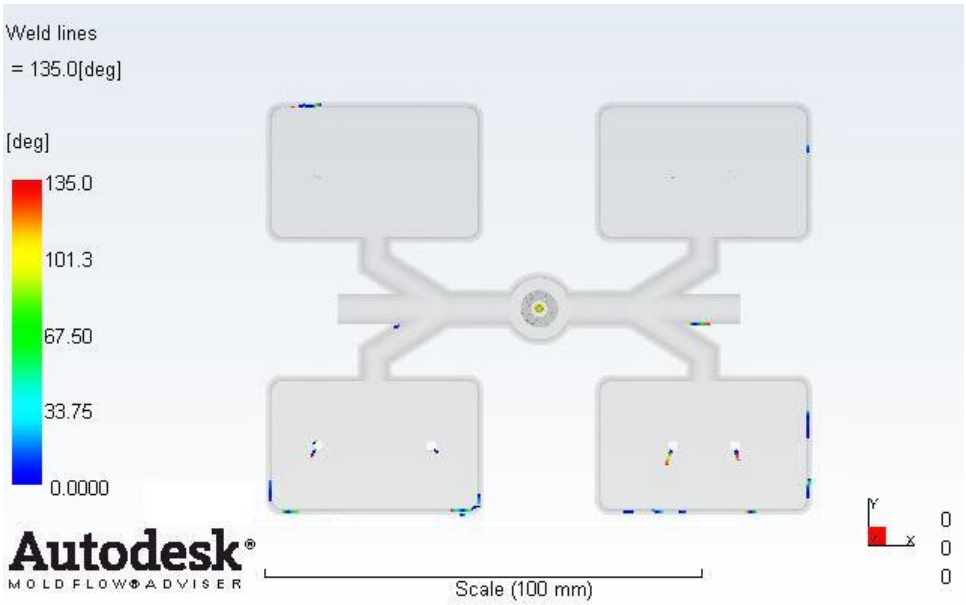

Figure 3.9: Weld lines

due to the mold design. However, the results are not symmetric, which might be due to numerical errors. This issue will be further discussed in Chapter 5.

(9) Temperature variance: The temperature variance result displays the effect of the shape of the product on the temperature distribution over the surface. Thick sections and heat traps, such as small enclosed areas, also affect the way that the polymer cools; hence, this result should be read in conjunction with the cooling time variance result [83]. The red color indicates the areas which are hotter than the average, and the blue color indicates the areas which are colder than the average [83]. The analysis result can be seen in Figure 3.10. It can be inferred from the analysis, temperature variance is symmetric and the surface of the product is colored in green (at average temperature) due to proper design of the mold. Therefore, the thickness of the product is suitable and there is no heat trap which can cause difference in cooling time for different regions. This issue is important to achieve low warpage for the product.

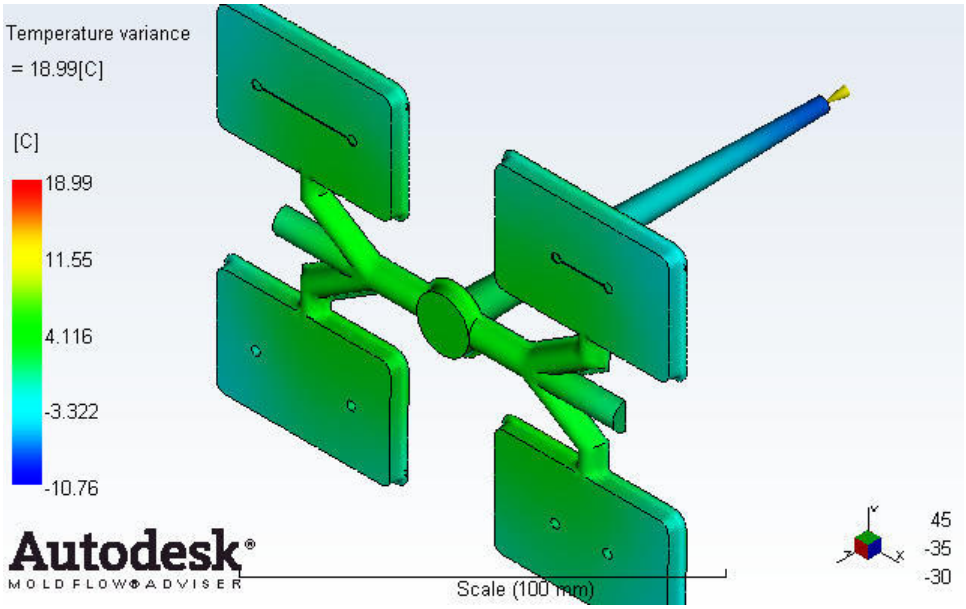

Figure 3.10: Temperature variance

(10) Cooling time variance: The cooling time variance analysis indicates the difference between the time takes for the polymer to freeze in any region of the part and the average time takes to freeze within the entire product [83]. Areas which are plotted as positive values, appeared in red color, take longer to freeze than the average freezing time and areas which are plotted as negative values, appeared in blue color, freeze more quickly than the average freezing time and zero values in this result point the average time to freeze [83]. Red color indicates that the area needs more cooling. The temperature variance analysis together with the cooling time variance analysis indicates the locations on the product that might require redesigning, such as modification of the thickness of a wall, an extension or modification of the existing cooling system [83]. The analysis result can be seen in Figure 3.11. There is only one red area in the analysis which is located at the end of the sprue. However, this area does not have any effect on the quality of the product. The cooling time variance for the product is low (blue in color in Figure 3.11). According to this analysis, in the view of the cooling of the product, the design is proper does not need any cooling system.

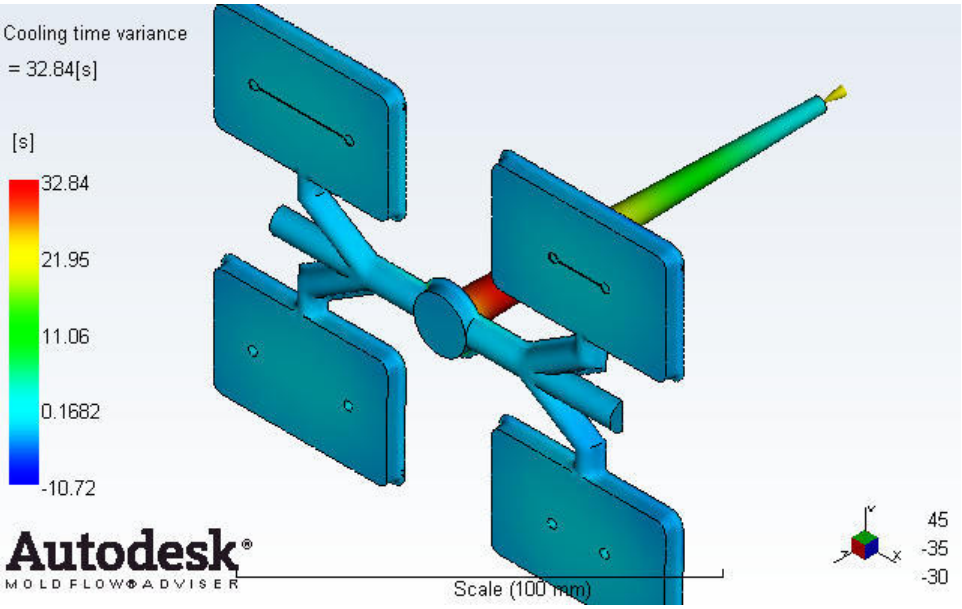

Figure 3.11: Cooling time variance

(11) Cooling quality: The cooling quality analysis indicates where the heat tends to stay in a part due to its shape and thickness [83]. The part is considered to be embedded in a large metal block with no cooling systems and the heat is assumed to be lost from the outer surfaces of the block. The cooling quality result is derived from the combinations of the temperature variance and cooling time variance results [83]. Each of these results divided into ranges that identify areas of the part where the design could lead to poor or low quality of cooling (red), medium quality cooling (yellow) and high quality cooling (green). The analysis result can be seen in Figure 3.12. It can be seen from the analysis that general cooling quality of the product is high (%86.5). There are red areas in the result (10%); however, areas in red color mainly are seen at the sprue side which does not have any effect on the quality of the product. On the other hand, according to the analysis, locally cooling problem may be experienced at the side walls of the product. Another possible reason for this may also be the numerical errors due to the very thin features, since although the design of the mold is symmetric, the red areas are not.

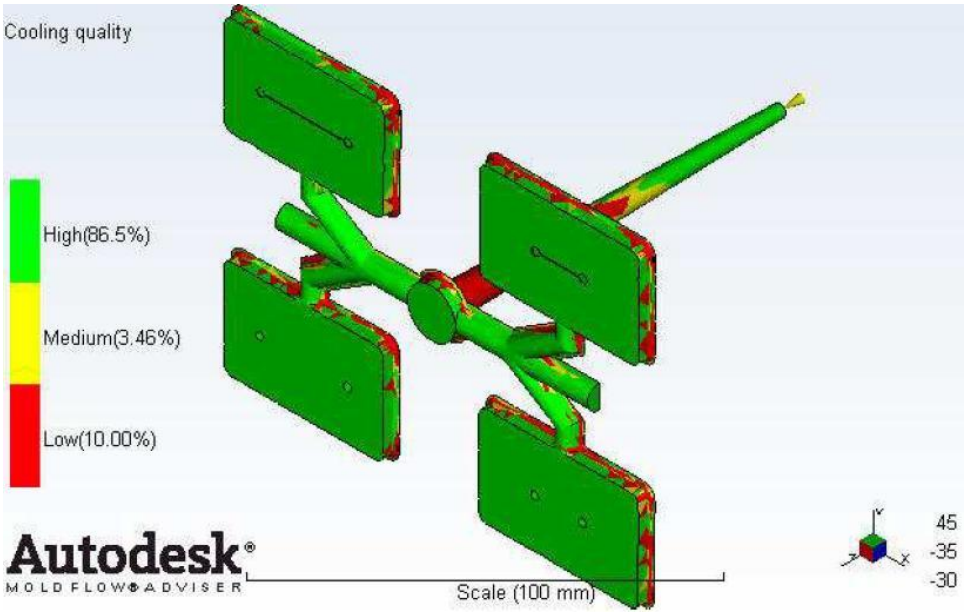

Figure 3.12: Cooling quality

(12) Volumetric shrinkage at the ejection: The volumetric shrinkage at the ejection analysis indicates the volumetric shrinkage for each area expressed as a percent of the original modeled volume [83]. Volumetric shrinkage needs be uniform across the whole part to reduce the warpage of the final product [83]. The analysis result can be seen in Figure 3.13. It can be seen from the analysis that uniform shrinkage is expected. Moreover, although the shrinkage of molded plastic parts can be as much as 20% by volume [84], low shrinkage is expected ($\sim$6%) at product due to the proper design of the mold. Due to the uniformity, low warpage of the final product is also expected.

(13) Warpage indicator, all effects: The warpage indicator, all effects analysis indicates those areas of the part where the out-of-plane deflections are approaching or exceeding the specified nominal maximum deflection (NMD) value [83]. Warpage occurs when there are variations of the internal stresses in the material caused by a variation in the shrinkage (non-uniform cooling and inconsistent shrinkage) [83]. Inconsistent shrinkage can be seen due to variations within the material (property variations, varying moisture content, inconsistent melt and pigmentation), variations in the process conditions (inconsistent packing and varying mold and melt temperatures) and variations within the molding

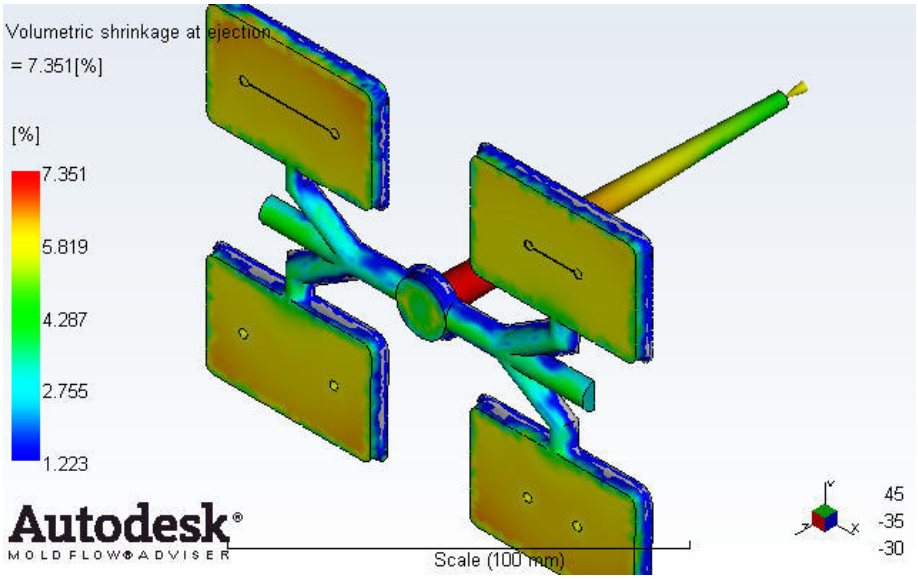

Figure 3.13: Volumetric shrinkage at ejection

machine (damaged check ring and unstable controller) [83]. The analysis result can be seen in Figure 3.14. It can be inferred from the figure that low warpage is expected due to the proper design of the mold. However, still certain amount of warpage can be expected in the final product due to the variations within the material and molding machine during the actual fabrication process.

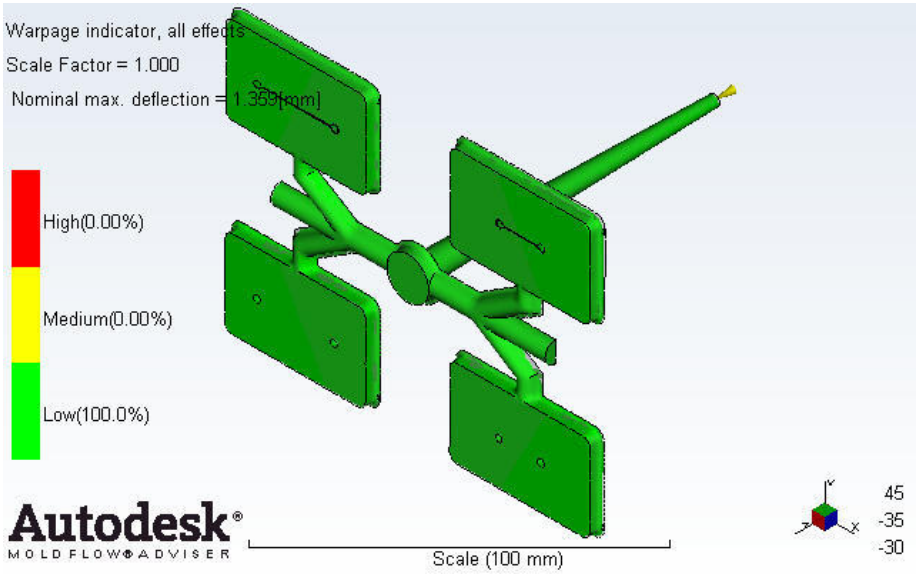

Figure 3.14: Warpage indicator, all effects

Table 3.3: Volumetric shrinkage and time to reach the ejection temperature for different mold temperatures

Mold Temperature [°C]	**Shrinkage** [%]	**Time** [s]
35	6.9	111
45	7.1	121
55	7.2	134
65	7.4	152
75	7.6	178
85	7.7	228

Moldflow® analysis was repeated for 35°C, 45°C, 55°C, 65°C, 75°C and 85°C mold temperatures to find the best mold temperature. Flow resistance, best gate location, fill time, confidence of fill, pressure drop, weld lines, temperatures variance, cooling time variance, cooling quality analyses showed the same results, since these analyses depend on only the designed mold geometry. Moreover, the warpage indicator analysis for different mold temperatures were found to be the same and all of results were 100% low. There were two analyses which showed differences at different mold temperatures: time to reach ejection temperature analysis and volumetric shrinkage at ejection analysis. These analyses' results can be seen in Table 3.3. According to volumetric shrinkage analysis, in order to get the minimum volumetric shrinkage, low mold temperature needs to be preferred during the injection. Moreover, increasing the mold temperature also increases the time to reach the ejection temperature. Hence, the cycle time needs to be adjusted with respect to the mold temperature.

Although the simulation tools use detailed models and ask for many input parameters during the simulations, the simulation models cannot cover all the physics of the injection due to the complex nature of the process. Therefore, the validity of the simulation results are questionable. Following the injection molding product, the simulations results will be assessed in Chapter 5.

Chapter 4

Manufacturing

4.1 Mold Manufacturing

Fabrication of the mold or the tool simply can be defined as the machining of negative or inverse of the desired pattern or geometry on the mold material. Once the fabrication of the mold is performed, then it can be used to replicate a the polymer substrate many times. This is an important aspect which offers substantial cost advantages. One another advantage is that molds can be manufactured with a large number of different fabrication methods including micro-fabrication techniques for micro-feartures [5]. Precision of the mold significantly determines the quality of the end product such as any surface defect on the mold will be replicated faithfully in the polymer product [5]. Moreover, the lifetime of the mold depends strongly on the surface quality of the mold. The smoother of the mold surface result in the lower the frictional forces during demolding [5]. For reliable high-quality replication, roughness of the mold should be less than 100 nm RMS [58]. Surface morphology, adhesion properties to the molded materials, lifetime, feature sizes, and costs are the critical factors to be considered for the manufacturing of the mold [5].

The fabrication of a mold with micro-features are even more challenging than the molds with macro-featrues. There are mold manufacturers specialized in

Table 4.1: Mold manufacturer specializing in molds with micro-features

Company	**Web Site**
ALC Precision, NY	www.alcprecision.com
Accumold, IA	www.accu-mold.com
Micromold, Inc. CA	www.micromoldinc.com
Makuta technics, IN	www.makuta.com
Precimold Inc. Canada	www.precimold.com
Rolla AG, Switzerland	www.rolla.ch
American precision Products, AL	www.injection-moldings.com
Sovrin Plastics, UK	www.sovrin.co.uk
Stack Plastics, CA	www.stackplastics.com
Stamm, Switzerland	www.stamm.ch
Rapidwerks	www.rapidwerks.com
Micro Precision Products, CA	www.microprecisionproducts.com

molds with micro-features. Some of these manufacturers are listed in Table 4.1. There are a number of methods which can be used to manufacture molds with micro-features. These methods can be classified in three groups:

(i) High-precision mechanical machining

(ii) Bulk micro-machining (eg., etching Si)

(iii) Surface micro-machining (eg., nickel electroplating in photoresist or LIGA molds)

(i) High-precision mechanical machining: New generation mechanical machining technologies are capable of producing features on the order of a few tens of micrometers with using high-precision fabrication machines such as computer numerical control (CNC) milling. One of the great advantages of

the micro-mechanical machining is that many materials can be machined, even stainless steel which offers excellent lifetime for molds can be machined which cannot be processed with any other micro-fabrication technique [5]. Relatively basic geometries with straight walls are a good fit for high-precision mechanical machining. However, structures which have high aspect ratios, very deep holes, or very small structures (less than 10μm) cannot be fabricated [5]. Moreover, with surface roughness around several micrometers, these techniques typically do not produce smooth surface finishes. High-precision mechanical machining is the best for the features, often greater than 50μm (with tolerances around 10μm) [58]. Structure with high aspect ration can be problematic in this method. However, nowadays aspect ratio 5 is achievable by the development of the new machining technologies [5]. Unlike other fabrication techniques, high-precision mechanical machining can be utilized for the fabrication of 3D structures without any problem. One drawback of the high-precision mechanical machining is that it requires high-precision machining machine and an operator assistance for the use of this machine.

(ii) Bulk micro-machining: In bulk micro-machining, the mold is created by etching a substrate wafer. Mostly silicon is used as the substrate since silicon is an excellent material for use as an embossing master [58]. It has a high modulus of elasticity and high thermal conductivity which are desired for hot embossing [5]. To fabricate a silicon master, these steps needs to be followed [5]:

(1) A pattern (mold) is created by using any CAD software and the created image is transferred to a photomask [54].

(2) Si wafer is coated with a masking material like silicon dioxide or silicon nitride.

(3) Coated Si wafer again coated with a layer of photoresist.

(4) UV exposure, the photoresist is used revealing the transferred image.

(5) The image is passing to the exposed masking layer by using either wet or dry etching.

The exposed silicon can be etched anisotropically by using potassium hydroxide (KOH), tetramethylammonium hydroxide (TMAH), or ethylenediaminepyrocatechol(EDP). Dry etching methods, like deep reactive ion etching (DRIE) and the Bosch process [54] can also be used to manufacture deep structures with vertical sidewalls [5]. However, scalloping or high surface roughness can be experienced due to the non-optimized or fast etches, which may cause problems during demolding. Although through holes have been achieved by using the Bosch process, the range of the depth achieved generally changes from 10 to 40μm, [5]. Although silicon molds are relatively simple to manufacture and they offer good resolution and surface properties, they have some disadvantages. To name few, they may be too fragile for typical hot embossing pressures and may require some form of reinforcement, they may also stick to polymers depending on their surface chemistry, which would decrease the number of possible replication cycles [5]. Moreover, clean room facility is necessary for the fabrication silicon molds.

(iii) Surface micro-machining: In the surface micro-machining, a mold is typically created by applying the following steps [5]:

(1) Coating of a wafer surface with a conducting seed layer by evaporation of sputtering.

(2) Deposition of a thick photoresist and patterning on a wafer surface.

(3) Electroplating of the pattern with nickel.

(4) Removal of the photoresist

(5) Etching of the seed layer.

This method is widely used for the production of molds for hot embossing and for injection molding. Surface micro-machining is commonly used since a nickel mold can be made with a low surface roughness, high durability, and a ability to replicate small and high aspect ratio features [5]. Conventional photo-lithography, X-ray or UV LIGA followed by electroplating nickel or nickel alloys on silicon or nickel substrates are also one of the widely used surface micro-machining techniques for the fabrication of molds with very small and complex features [85–87].

Table 4.2: Comparison of the manufacturing methods [3]

Method	**Size**	**Tolerance**	**Aspect Ratio**	**Roughness**
Ion Beam LIGA/2D	0.1–0.5μm	0.02–0.5μm	1	n/a
Focused Ion Beam LIGA/3D	0.2μm	0.02μm	n/a	n/a
X-Ray LIGA/2D	0.5μm to 1mm	0.02–0.5μm	10–100	$< 20nm$
Electron Beam LIGA	0.1–0.5μm	n/a	1–2	n/a
UV LIGA/2D	2-500μm	n/a	1–10	n/a
Femtosecond laser/3D	1μm	<1 μm	1–10	n/a
Excimer laser/3D	6μm	<1μm	1–10	1 μm - 100 nm
Ultra short pulse ECM/3D	Few μm	<1 μm	8	n/a
Micro EDM/3D	10–25μm	3μm	10–100	0.3-1 μm
Micromilling/3D	25μm	2 μm	10–50	Few Microns
Deep UV resists	n/a	2–3μm	22	$\sim$1μm
Deep reactive ion etching	n/a	<1 μm	10–25	2 μm

Although electroplated nickel surface is very smooth and compatible with most polymers, electroplating of tall, high aspect ratio structures may require very long exposure time. To speed up the process the current density may be increased, which may result in the increase of the stress levels and the surface roughness [5].

Comparison of the different manufacturing methods for the mold is listed in Table 4.2 (adapted from [3]).

4.1.1 High-precision mechanical machining of the mold

In this study, for the manufacturing of the mold, High-precision mechanical machining method is used considering the aforementioned advantages. Blank (unmachined) mold system was supplied by Güvenal Teknik Hırdavat Tic. San. Ltd. Şti. [88]. The mold was fabricated by using the high precision CNC facility (Model: Deckhel Maho DMU 50) of Bilkent University Micro System Design and

Table 4.3: Tool list used in machining of the mold

Tool	**Diameter**	**Min. Cutting Lenght**
Carbide end mill	1 mm	3 mm
Carbide end mill	4 mm	3 mm
Carbide end mill	4 mm (R0.5)	3 mm
Carbide end mill	8 mm	3 mm
Carbide ball nose	4 mm	3 mm
Carbide ball nose	6 mm	3 mm

Manufacturing Center. The mold material was chosen as stainless mold steel (CK–50 AISI 1.1050). In the machining process, four teeth coated carbide tools were preferred. Tools used in the machining of the mold are listed in Table 4.3. Carbide ball nose was used for the machining of the runner and the gate. Carbide end mill (straight and rounded) was used for the mold cavity. For the machining of the mold, the required G-Codes were generated in SolidCAM software. Since the mold geometry includes side walls with a draft angle and ball shaped runner and gate, 3D CAM was necessary. Spindle speed and feed rate required for the machining were calculated by the following equations respectively:

$$N = \frac{1000 \times V_c}{\pi \times D}, \tag{4.1}$$

$$V_f = f_z \times z \times N, \tag{4.2}$$

where, N [rpm] is the spindle speed, V_c [mm/min] is the suggested cutting speed by the manufacturer of the tool, D [mm] is the diameter of the tool, f_z [mm/tooth] is the feed per tooth V_f [mm/min] is the feed rate, z is the number of teeth. According to the chip formed during the machining; the feed rate and spindle speed were adjusted by the operator. First, the runner, gate and mold cavities were roughly machined, and the base and side walls were machined with

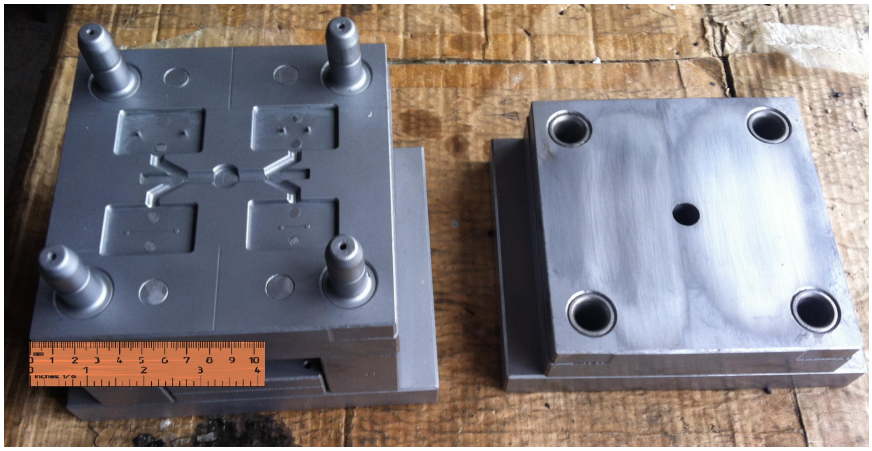

Figure 4.1: Photograph of the mold after machining

0.5 mm tolerance. Then, the tolerances and tool diameters were decreased after each pass. The machining of the mold took nearly four hours. The machined mold can be seen in Figure 4.1. After the micro-mechanical machining of the mold, in order to increase the surface quality, a surface finish operation was performed by using a grinding machine and special pastes. Photograph showing the grinding opretation can be seen in Figure 4.2. To check the accuracy of the machining, the dimensions of the microchannel structures within the mold were measured using optical measurement microscope (Vision Engineering Hawk 200). The accuracy of the dimensions were found to be within $\pm 5\mu$m.

Figure 4.2: Photograph showing the grinding operations

4.2 Injection Molding of the Microchannels

Proceeding the manufacturing of the mold, the injection molding of the microchannels were performed. The injection was performed in Modern Teknik Plastik San. Tic. company (OSTİM, Ankara). Üçel plastic injection molding machine was used. The photograph of the injection machine can be seen in Figure 4.3. It was 1980 model and its maximum injection pressure is 90 MPa. The machine has two heaters; one for melting the injection material and the other for adjusting the mold temperature. Injection molding was performed with six different mold temperatures: 35°C, 45°C, 55°C, 65°C, 75°C and 85°C in order to find the best injection temperature in terms of warpage of the product. The melting temperature of the plexiglas (245°C) and the injection pressure (90 MPa) were kept constant during the injection experiments. Only the mold temperature was varied during the injection. In order to monitor the mold temperature precisely, an external thermocouple was installed. To install the thermocpouple, a hole was drilled as close as possible to the mold cavity. Then, the thermocouple was inserted into the hole. During the injection experiment, only the mold temperature was monitored. The scene for the monitoring of the temperature during the experiments can be seen in Figure 4.4.

Figure 4.3: The photograph of the injection machine

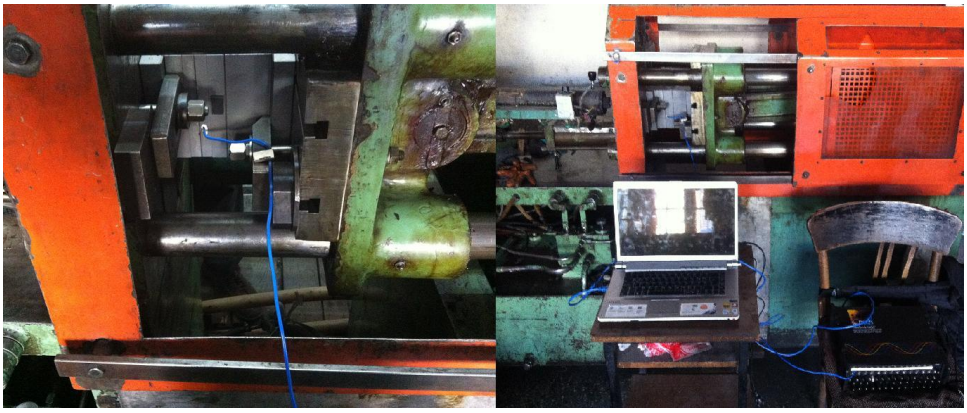

Figure 4.4: Scene for the monitoring temperature during the experiment

Prior to the experiment, polymer material (Plexiglass 6N) was put into the oven and kept at 90°C for 120 minutes to remove humidity. If the material is not dry enough, the surface quality of the end product will not be good, and air bubbles might also be experienced inside the product. The experiments were conducted starting from the high mold temperatures (85°C) and moving to the low mold temperatures (35°C). Inner heater of the plastic injection molding machine was adjusted to 85°C. A flame gun as an external heater was also used on the mold to assist the heating of the mold. When the injection started, the temperature was read about 90°C. During the injection, the temperature dropped. After a while, at 84.2°C (±0.4°C), the mold temperature reached the quasi steady-state condition (due to the injection and ejection of the product temperature changes in a cyclic manner even at steady-state conditions). Then, the samples associated with this mold temperature were collected. Unfortunately the temperature of the mold was not be able to be held at steady-state condition for a long time. Only nine samples were able to be collected for the mold temperature of 84.2°C. A representative temperature curve showing the mold temperature can be seen in Figure 4.5 (steady-state regime for the operation is also labeled on the figure). Injection cycle took about 22 seconds at the mold temperature of 84.2°C. Although the product itself was cooled enough and rigid, the injected parts at the sprue side was observed to be hot and pliable after the demolding. The experiments were repeated for other mold temperatures by following the same procedure. Steady-state temperatures, the number of collected samples and respective cycle time are tabulated in Table 4.4. For low mold temperatures,

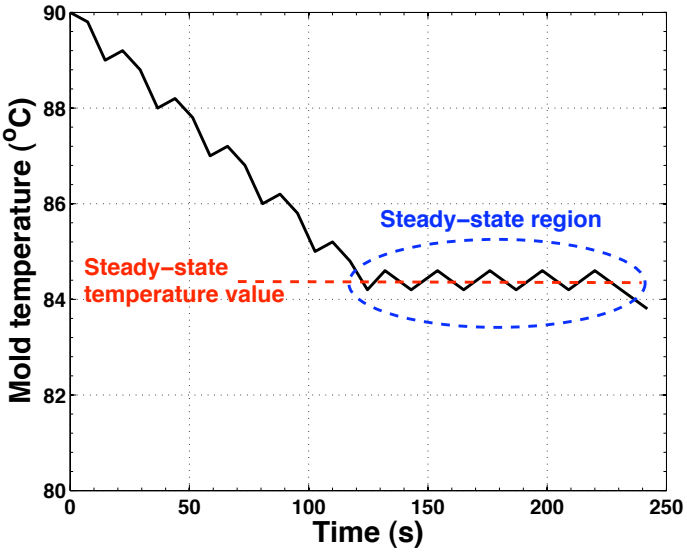

Figure 4.5: Representative figure for the temperature of the 85°C during the injection

steady-state temperatures were over the adjusted temperature. Unlike the other mold temperature experiments, steady-state condition of 35°C mold temperature experiment was broken due to the increasing temperature. For 45°C and 55°C, the heater of the injection molding machine was able to keep the steady-state condition without any problem. Therefore, more samples were collected at the aforementioned temperatures.

Experiment photos can be seen in Figure 4.6. In the first picture, external heater (flame gun) application can be seen and the second picture was taken during the demolding process.

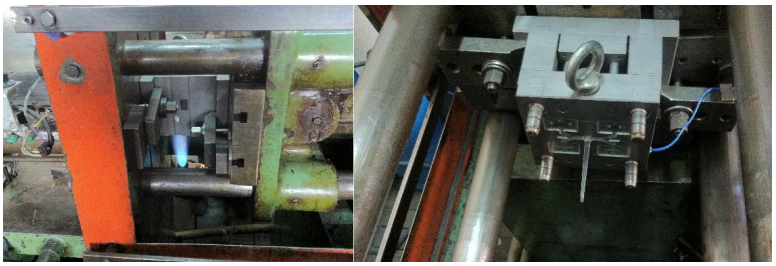

Figure 4.6: Photograph of the experiment

Table 4.4: Number of samples collected and cycle times for different mold temperatures

Mold Temperature [°C]	**Actual Temperature [°C]**	**Number of Samples**	**Average Cycle Time [s]**
35	36.2 (±0.5)	15	12
45	45.6 (±0.5)	30	13
55	55.4 (±0.5)	30	15
65	64.7 (±0.4)	18	18
75	74.7 (±0.4)	12	20
85	84.2 (±0.4)	9	22

4.3 Bonding of the Microfluidic Device

Following the production of the microchannels by injection molding, in order to transform the microchannels into real a microfluidic device, the top side of the channels needs to be covered to prevent any leakage during the fluid flow. Generally methods to bond polymeric pieces can be listed in four groups: Anodic bonding, direct bonding, adhesive bonding and eutectic bonding [2].

(i) Anodic Bonding: Anodic bonding is one of the oldest bonding technique in silicon-based micro-machining [2]. This technique is used to bond a glass substrate to a silicon substrate. General conditions for the anodic bonding are the temperature on the order of 400°C and the high electrical field with bonding voltage about 1 kV [2]. Silicon is attached to the positive electrode and behaves as an anode, which gives the name to this method [2]. Anodic bonding causes a large temperature variation to the glass/silicon stack. If the thermal expansion coefficients of glass and silicon do not match or not close enough, the stress upon cooling causes cracks, it can be seen in either silicon or glass [2]. Therefore, the glass substrate must be matched with the thermal expansion coefficient of the

silicon wafer. Examples of suitable glasses for this aim are Corning 7740 (Pyrex), Corning 7750, Schott 8329, and Schott 8330 [2]. Anodic bonding can also be used to bond two silicon layers by coating a thin glass layer on top of one of the two substrates. The bonding process works as usual with the glass-covered silicon wafer replacing the glass substrate. Due to the optical transparency of the glass, anodic bonding technique is commonly used for the fabrication of micromixers for biochemical applications in which optical access for manipulation and evaluation of the fluid are needed [2].

(ii) Direct Bonding: Direct bonding technique is applied to bond two substrates of the same material. It can be used on various materials such as silicon, glasses, polymers, ceramics, and metals [2]. Direct bonding, also called fusion bonding, directly bonds materials of same kind under high temperature. The advantage of this technique is the lack of thermal stresses due to the perfect matching of the thermal expansion coefficient of the two substrates [2]. The bonding process for silicon wafers is typically occured at temperatures between 300°C and 1000°C [2]. Annealing the bonded stack at high temperatures (800°C to 1100°C) promotes the bonding quality [2]. Direct bonding between glasses is called glass to glass bonding. Two glass wafers can be thermally bonded/sealed together at 600°C for 6 to 8 hours [89]. Many polymers can also be directly bonded/sealed at temperatures which is above their glass transition temperatures (T_g) [2]. In the case of polymers with low surface energy, like PDMS, a surface treatment with oxygen plasma can also seal the two polymer materials at room temperature [2].

(iii) Adhesive Bonding: Adhesive bonding can be briefly explained as the bonding of substrates by the help of an intermediate layer (glue). Depending on the substrates and application, the intermediate layer can be glass, epoxies, photoresists, or other polymers; such as, a thin intermediate glass layer can thermally bond to silicon substrates [2]. Annealing of the pack at sealing temperatures causes the glass (intermediate) layer melt and flow [2]. Then, cooling down to room temperature gives a quality bonding between two substrates [90]. Moreover, a number of epoxies [91], UV-curable epoxies [92], and photoresists can also be used for adhesive bonding; such as, SU-8 is used in many microfluidic applications for adhesive bonding as intermediate layer [2]. The main advantages of

using polymers as an intermediate layer (glue) is the low process temperature [2] and it is not limited to only silicon substrates, it can be used for any kind of substrate material [2].

(iv) Eutectic Bonding: In eutectic bonding, eutectic metals (which transform directly from solid to liquid state, or liquid to solid state, at a specific composition and temperature without passing a two-phase equilibrium) are used as an intermediate layer. Eutectic bonding is commonly used in packaging of the electronic circuits. For example, a thin gold film can be sputtered on the silicon wafer for this purpose, then eutectic bonding is occurred at a relatively low temperature of 363°C [2].

In this study, direct bonding and adhesive bonding methods were used to bond the plexiglas microchannels.

4.3.1 Direct Bonding of the Microfluidic Device

In the direct bonding method, it is very critical to align microchannels on reservoirs. For this purpose, a lock mechanism was designed. Moreover, a lock mechanism also supplies the pressure to help bonding. The photograph of the lock mechanism can be seen in Figure 4.7. Direct bonding occurrs above the glass transition temperature of the polymer. Glass transition temperature of plexiglas's is 110°C. Therefore to find the optimum temperature for the direct bonding, many temperatures were tried. Trials were started from 120 °C for 15 minutes. However, direct bonding did not occur at this temperature; hence, the temperature was increased step by step while the time was kept constant. Direct bonding successively reached at 140°C for 15 minutes. Direct bonding may also be achieved at higher temperature by keeping the product less than 15 minutes However, higher oven temperatures may also deform the microchannel structure.

Figure 4.7: Photograph of the lock mechanism

4.3.2 Adhesive Bonding of the Microfluidic Device

In the adhesive bonding method, a solvent is required. Chloroform, which is a solvent for plexiglass, was used for the adhesive bonding. During the adhesive bonding, the critical issue is that the solvent should not deform the microchannel. In order to protect the microchannel, the microchannel was covered with a chemical, %2 sodium alginate. This chemical does not react with the solvent, and at the same it is dissolvable by water. First, the microchannel was filled with sodium alginate and it was put into the refrigerator. When sodium alginate was frozen, it expanded and completely filled the microchannel. Then, chloroform was applied to the top surface of the microchannel. After that, other plexiglas which has the reservoir openings was closed on top of the surface where chloroform applied. Reservoir alignment is also critical in the adhesive bonding. The bonding was achieved in a minute. After the bonding, water was injected into the microchannel to dissolve sodium alginate. The process took nearly 30 minutes. Experiment photos can be seen in Figure 4.8. Compared to direct bonding method, this method is more time consuming relatively more labor-intensive. Moreover filling process of the microchannel with sodium alginate, the application of chloroform on the surface and the reservoir alignment are the challenging processes associated with this method. Due to these reasons, it was concluded that

Figure 4.8: Application of the sodium alginate

direct bonding method is more suitable for the mass production of the microfluidic devices. Therefore, direct bonded microchannels were used in the bonding quality tests.

Chapter 5

Results and Discussion

In chapter 3, different analyses were performed by using Moldflow® simulation tool. After the injection experiments, the results were compared with the simulation results.

5.1 Assessment of the Simulation Results

Filling: According to simulation results such as confidence of fill, pressure drop, gate location and flow resistance analysis, smooth and full-filling of the mold was expected. During the injection, there were not experienced any filling problems. The easiest way to check the full-filling is to examine the air vents, since the air vents are located at the end corners of the mold cavity. In our design, filling of the the air vents with the polymer material ensures the filling of the mold cavity. Filled air vents highlighted by red circle (cracked during the demolding) can be seen in Figure 5.1.

Weld lines: According to weld line analysis, the weld lines were expected near the reservoirs. After the injection molding, the weld lines were observed at the expected areas. The weld lines highlighted by green circle can be seen in Figure 5.1. However, the weld lines are found to be nearly symmetric unlike the

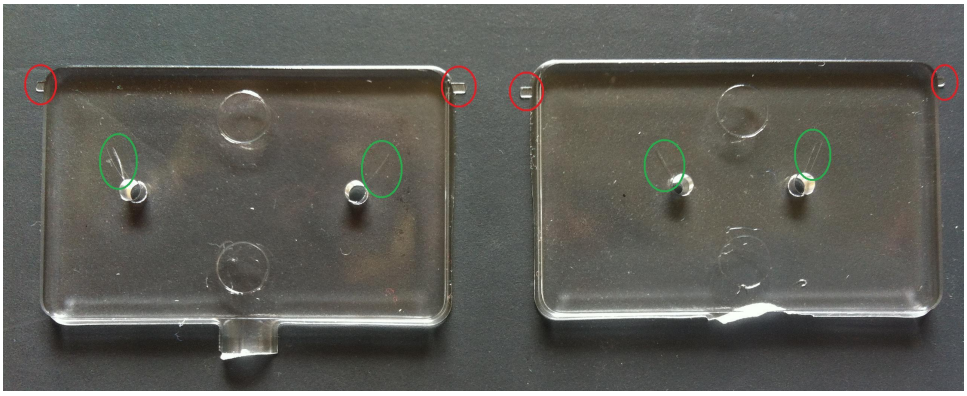

Figure 5.1: Injected plexiglas

simulation results. This inconsistency may be the result of a numerical error in the simulations.

Demolding: According to draft angle analysis, demolding was expected to be easy. During the injection molding, products were easily removed from the mold without any need for a release agent as expected. Moreover, it was observed that the pushing pins helped the demolding process as expected.

Cycle time: The measurement results of the cycle time from the experiments are shown in Figure 5.2. The simulated time to reach the ejection temperature for different mold temperatures are also given in the same figure. Actually, to get the cycle-time for the simulated case, the fill-time and packing time needs to be added up to the time to reach the ejection temperature. As seen from the figure, even the time to reach ejection temperature is much higher than the experimental cycle times. Reason for this is that in the simulations, the time to reach the ejection temperature is calculated to ensure the complete cooling of the sprue. It was observed during the injection molding of the products, the cycle time used actually was low to ensure the complete cooling of the sprue. However, in a practical application, the cooling of the sprue does not affect the quality of the final product, so there is no need to wait for the sprue to be cooled. It was also the case in this study. Although the cycle time was not enough to ensure the complete cooling of the sprue, it was enough to ensure the complete cooling and the solidification of the product.

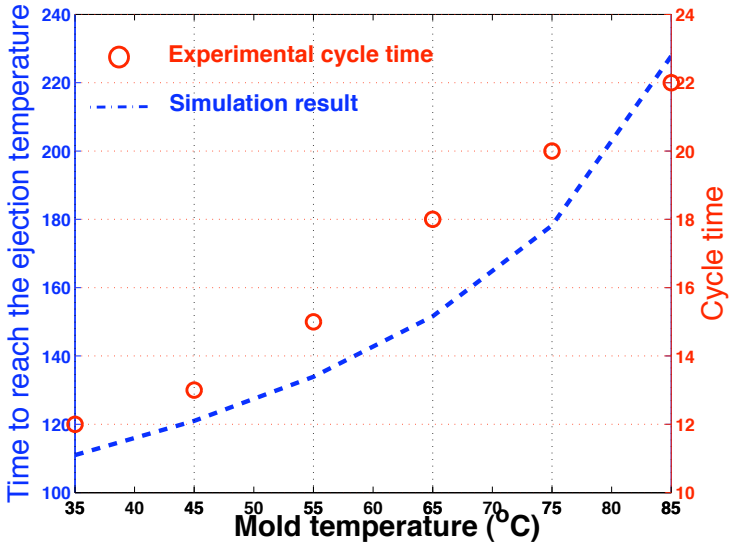

Figure 5.2: Comparison of the experimental cycle time and simulated time to reach ejection temperature

Although the scale of the simulation and the experimental results in Figure 5.2 are different, they have similar characteristics. The important conclusion which can be derived from these results is that as the mold temperature increases, the cycle time needs to be increased as well accordingly to ensure the demolding of the products without any deformation. If the cycle time was not sufficiently long enough, the products might be deformed by the pushing pins due to the insufficient solidification/cooling.

Warpage: According to the temperature variance, cooling time variance, cooling quality and warpage analyses, low warpage of the final product was expected. To characterize the warpage, measurements were performed using VK-X100 3D laser microscope. The photograph of the microscope can be seen in Figure 5.3. For each mold temperature, randomly selected six samples were measured. To characterize the warpage, following procedure was followed for each sample:

(1) A scan window was defined as an input parameter to the software (a typical scan window can be seen in Figure 5.4, 16 mm×3 mm)

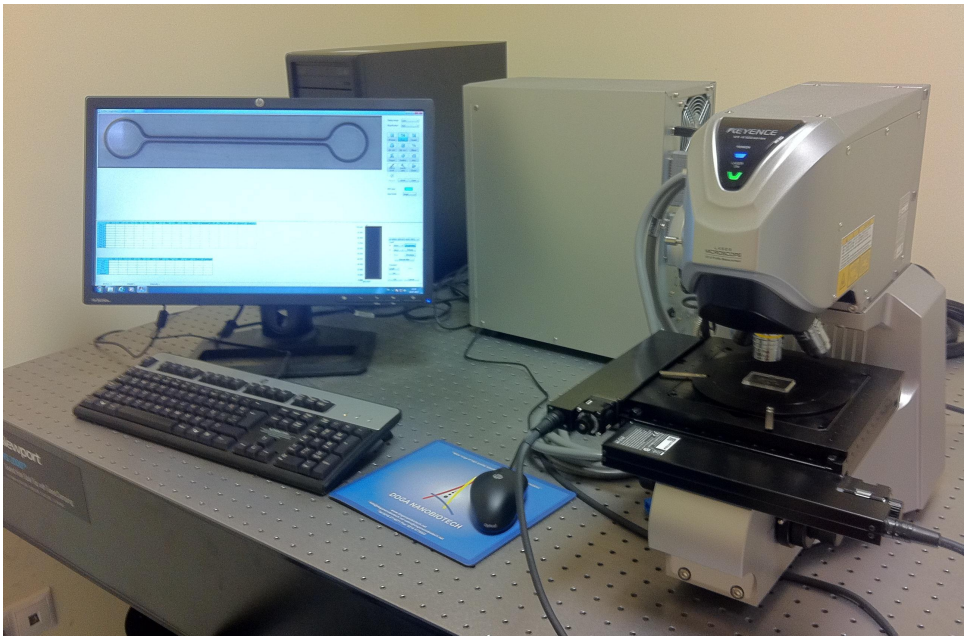

Figure 5.3: VK-X100 3D laser microscope

(2) The surface area within the scan window was scanned and the surface profile is digitized for the post processing by the software of the microscope (which took approximately 40 minutes).

(3) For the warpage measurement, several lines parallel to each other was generated by the software. The location of these lines were selected in accordance with the area where the measurements wanted to be taken (these lines can be seen as blue areas in Figure 5.4, actually these blue areas are composed of several lines). Different number of lines were selected for $x-$ and $y-$directions. 70 and 1000 lines were generated $x-$ and $y-$directions, respectively.

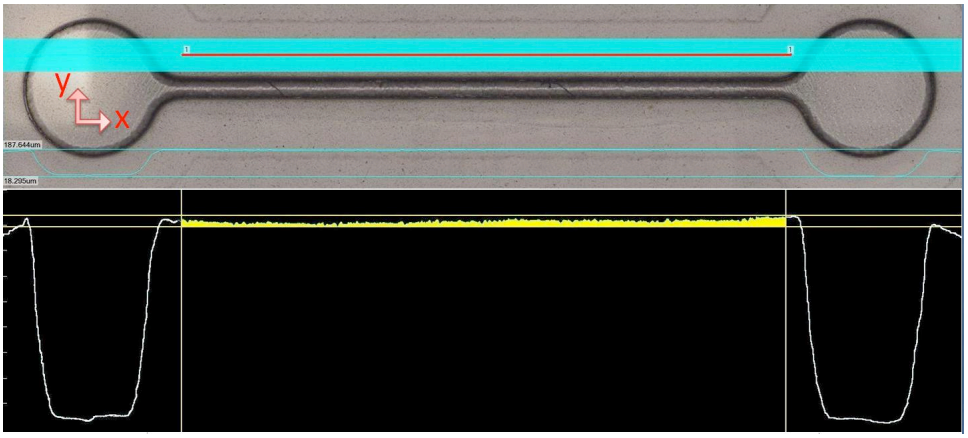

(a)

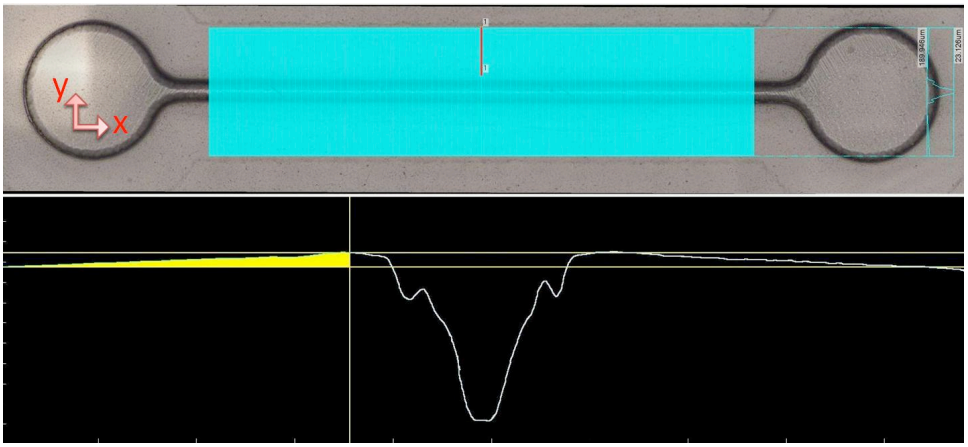

(b)

Figure 5.4: Measured area for the upper side: **(a)** $x-$direction, **(b)** $y-$direction

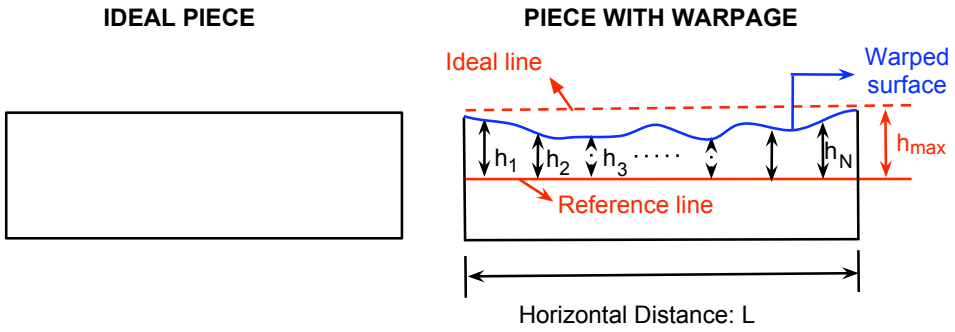

Figure 5.5: Schematic drawing to show the parameters in the characterization of the warpage

(4) To restrict the measurements at the upper and the lower sides of the microchannel, a line needs to be defined. The defined lines for the measurements in $x-$direction for the upper side of the microchannel can be seen as a red line on Figure 5.4-(a). The selected line for the measurements in $y-$direction for the upper side of the microchannel can be seen as a red line on Figure 5.4-(b).

(5) The software determines the average profile of the generated lines. The yellow area shows the shaded area between the line (indicating the average profile of the surface) and a reference line (arbitrary selected, see the schematic drawing in Figure 5.5).

(6) The software calculates the area of the yellow area (see the column "*C.S. area*" in Table 5.6) which depends on the selection of the reference line (which is the area between the blue line and the solid red line in Figure 5.5).

(7) The average height of the yellow area (h_{avg}) was calculated by dividing the yellow area by the horizontal distance, L which can be seen in Figure 5.5 and listed in the output table in Figure 5.6 (second column).

(8) To characterize the warpage, a parameter called *part deformation* was defined as the difference between the height difference (the difference between the ideal line (line correspondance to zero warpage) and the reference line which is indicated by h_{max} in Figure 5.5) and the h_{avg}. h_{max} listed in the output table in Figure 5.6 (third column).

	Horz. dist.	Hght. diff.	Hght. ave.	Angle	C.S. length	C.S. area	R
All	15140.0···	20.702um	70.433um	0.078°	15407.0···	1066653···	
Seg.1	9696.81···	9.675um	81.054um	0.057°	9729.65···	354148···	
Seg.2							
Seg.3							
Seg.4							

Figure 5.6: A typical tabulated output given by software of the microscope

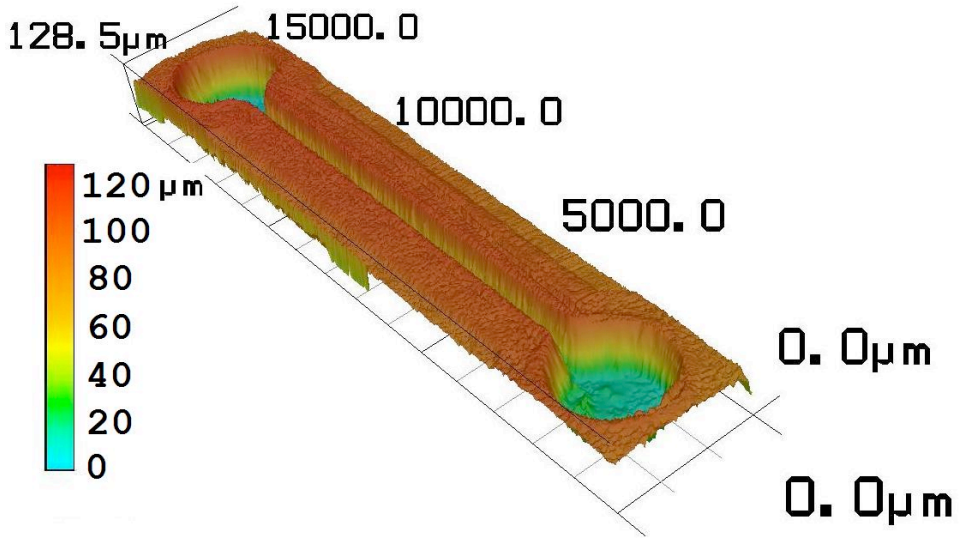

Figure 5.7: 3D part image

A typical tabulated output of the software can be seen in Table 5.6. Microscope also can create 3D part image to show all the height differences and the locations in $x-$ and $y-$directions (see Figure 5.7). Part deformations of the measured samples which were produced at different mold temperatures and the average of the part deformation of the samples for different directions are given in Tables 5.1–5.4. To characterize the overall warpage of the samples the average of the measurements at upper and bottom sides in $x-$ and $y-$ directions were calculated, which can be seen Figure 5.8 for different mold temperatures. The software outputs for each sample are given in the Appendix. It can be seen from the Figure 5.8 is that the minimum part deformation (4.96 μm) was occurred at the mold temperature of 45°C. The minimum part deformation is very important for strong direct bonding. It can be concluded that the ideal mold temperature is 45°C in terms of part deformation for the designed mold cavity. However, Moldflow® simulation advised 79°C (molding window analysis). It can be concluded that although Moldflow® simulation is useful for many analyses which were mentioned above, it cannot predict the best mold temperature for injection molding of the products with micro-features.

Table 5.1: Part deformation in $x-$direction (upper side of the microchannel)

Mold Temperature [$\circ$C]	**1**	**2**	**3**	**4**	**5**	**6**	**Average [μm]**
36.2 ($\pm$0.5)	9.270	9.072	8.019	7.709	8.530	8.448	8.51
45.6 ($\pm$0.5)	4.628	4.979	2.561	5.037	4.728	4.552	4.41
55.4 ($\pm$0.5)	13.429	16.539	13.083	11.395	13.625	12.671	13.46
64.7 ($\pm$0.4)	17.744	18.095	20.090	23.307	22.614	17.844	19.95
74.7 ($\pm$0.4)	25.999	33.178	34.282	27.758	27.681	26.660	29.26
84.2 ($\pm$0.4)	37.019	26.680	44.865	31.076	33.210	33.742	34.43

Table 5.2: Part deformation in $x-$direction (bottom side of microchannel)

Mold Temperature [$\circ$C]	**1**	**2**	**3**	**4**	**5**	**6**	**Average [μm]**
36.2 ($\pm$0.5)	5.441	6.999	5.749	7.628	6.023	7.596	6.57
45.6 ($\pm$0.5)	5.934	5.614	2.870	6.016	3.925	5.202	4.93
55.4 ($\pm$0.5)	13.378	16.787	11.330	11.067	11.938	13.443	12.99
64.7 ($\pm$0.4)	16.199	17.416	19.810	20.034	20.439	19.178	18.85
74.7 ($\pm$0.4)	20.212	24.386	31.434	23.837	24.418	26.660	25.16
84.2 ($\pm$0.4)	36.962	27.429	33.672	26.667	31.602	52.748	34.85

Table 5.3: Part deformation in $y-$direction (upper side of microchannel)

Mold Temperature [$\circ$C]	**1**	**2**	**3**	**4**	**5**	**6**	**Average [μm]**
36.2 ($\pm$0.5)	7.012	6.856	10.357	6.826	8.600	13.265	8.82
45.6 ($\pm$0.5)	6.358	5.466	2.730	5.850	4.811	6.542	5.29
55.4 ($\pm$0.5)	11.229	11.042	15.233	17.295	16.154	13.278	14.04
64.7 ($\pm$0.4)	20.627	23.943	20.717	20.708	22.450	19.062	21.25
74.7 ($\pm$0.4)	35.165	28.883	32.111	31.477	27.827	32.707	31.36
84.2 ($\pm$0.4)	34.056	46.421	43.364	47.762	49.768	45.861	44.54

Table 5.4: Part deformation in $y-$direction (bottom side of microchannel)

Mold Temperature [$\circ$C]	**1**	**2**	**3**	**4**	**5**	**6**	**Average [μm]**
36.2 ($\pm$0.5)	7.834	9.353	12.282	8.957	8.398	8.956	9.30
45.6 ($\pm$0.5)	4.606	6.186	4.298	5.065	5.455	5.602	5.20
55.4 ($\pm$0.5)	15.426	11.897	13.526	18.084	14.981	16.057	15.00
64.7 ($\pm$0.4)	20.556	19.357	24.253	19.754	23.318	21.596	21.47
74.7 ($\pm$0.4)	28.396	25.054	26.869	29.021	23.590	30.812	27.29
84.2 ($\pm$0.4)	39.767	33.174	34.005	35.538	33.882	37.988	35.73

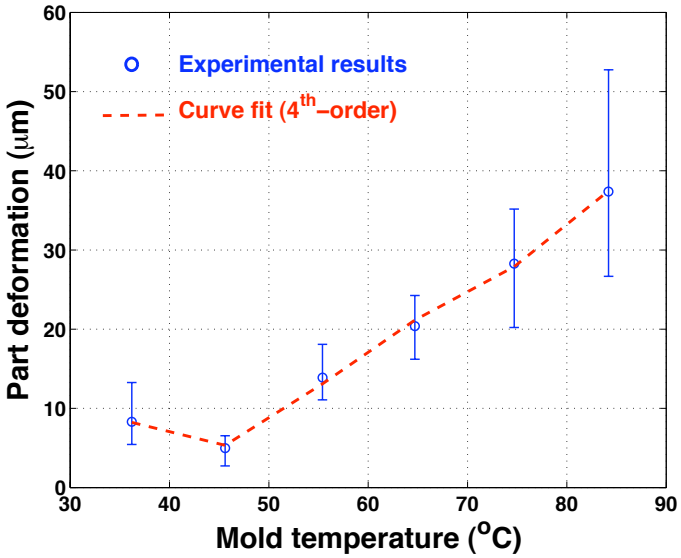

Figure 5.8: Overall part deformation

5.2 Bonding Quality Test of the Microfluidic Device

In order to relate the bonding quality to the warpage, bonding quality tests were performed. For the bonding quality tests, the microfluidic devices bonded with direct bonding were used. Bonding quality were checked by the injecting the pressurized water into the microchannel. The breaking pressure of the microfluidic device used as the indicator of the bonding quality. In order to prepare the experimental set-up, connection elements (capillary tube and its housing) were inserted into the reservoirs of the microchannel and sealed with epoxy. Bonding quality of the microfluidic device was measured in terms of the breaking pressure of the bond. The water within the microchannel was pressurized by means of a micro-pump (Model: Shimadzu corporation, LC-10ATVP). In the experiments, for each mold temperature, three samples were used. Flow rate of the micro-pump was increased step by step until the bonding was broken. Once the microchannel is broken, the pressure of the system drops somewhere near atmospheric pressure

which can be monitored over the display of the micro-pump. The experimental setup can be seen in Figrue 5.9. Breaking pressure for each sample and the average of these samples are listed in Table 5.5, and plotted in Figure 5.10.

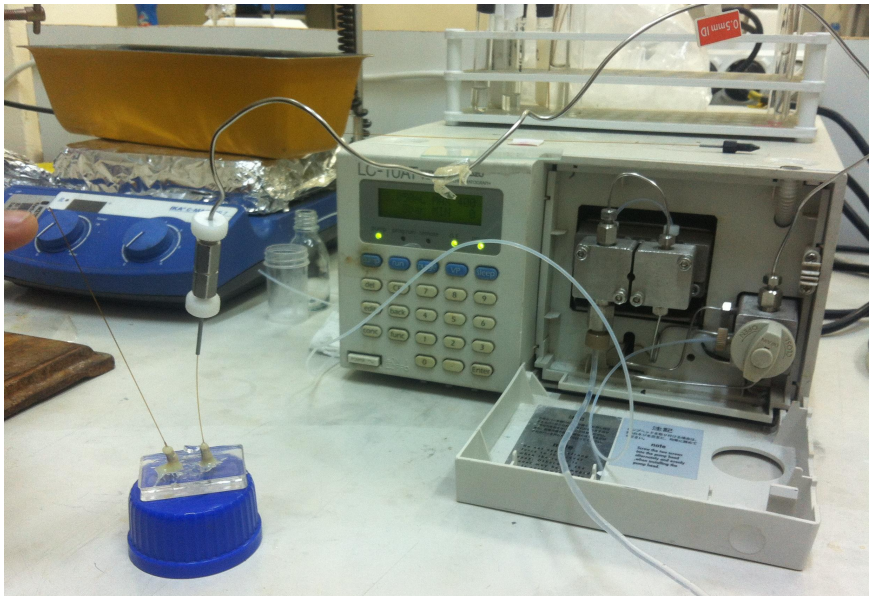

Figure 5.9: Experimental set-up

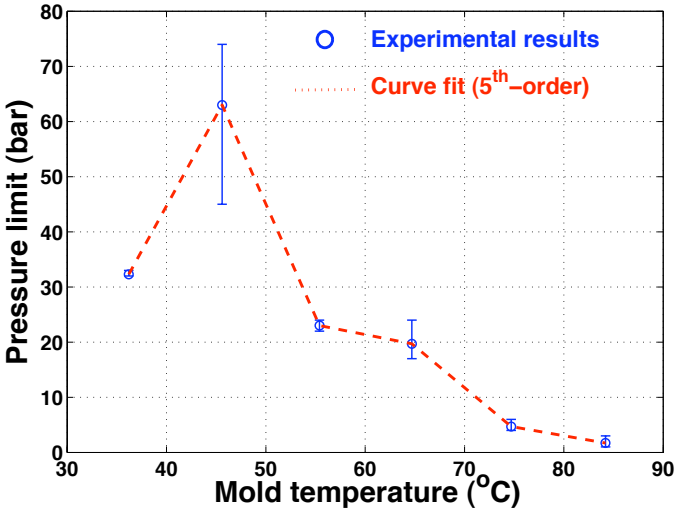

Figure 5.10: Breaking pressure of the bonding for different mold temperatures

It can be seen from the results, the stronger direct bonding was achieved when the microchannels were produced at a mold temperature of 45°C. According to the

Table 5.5: Bonding quality experiment results

Mold Temperature [°C]	**Sample#1 [bar]**	**Sample#2 [bar]**	**Sample#3 [bar]**	**Average [bar]**
36.2 (±0.5)	32	32	33	32.3
45.6 (±0.5)	70	74	45	63.0
55.4 (±0.5)	23	24	22	23.0
64.7 (±0.4)	17	24	18	19.7
74.7 (±0.4)	4	4	6	4.7
84.2 (±0.4)	1	3	1	1.7

warpage measurements (Figure 5.8), the minimum part deformation can also be seen at a mold temperature of 45°C. In addition to that, the trend of the bonding quality results shows a similarity to that of warpage measurements. Therefore, it can be concluded that there is one-to-one correspondence between the bonding quality and the warpage. The bonding quality increases with the decreasing warpage. There exists an maximum quality for the product which is achieved at the same mold temperature where the minimum part deformation is located. In terms of bonding quality, the corresponding mold temperature can be named as the optimum mold temperature. Maximum breaking pressure of 74 bars was achieved at the optimum mold temperature. The bonding between PDMS and glass/PDMS can withstand up to 5∼15 bars. Compared to the PDMS bonding, the current results are very promising especially when the HPLC applications are considered in which pressures around 50 bars are generated.

After the bonding quality experiment, leakage test was performed. In order to check the leakage, sample which was produced at a mold temperature of 45°C was used. The flow rate of the micro-pump was adjusted to a value less than the breaking flow rate (2 ml/min). In this flow rate, the pressure was observed as 70 bar. Then, the pressurized water flowed couple of minutes within the microchannel. Following these operations, a blue ink manually was injected into the microchannel and flow pattern of the ink was examined to check any possible

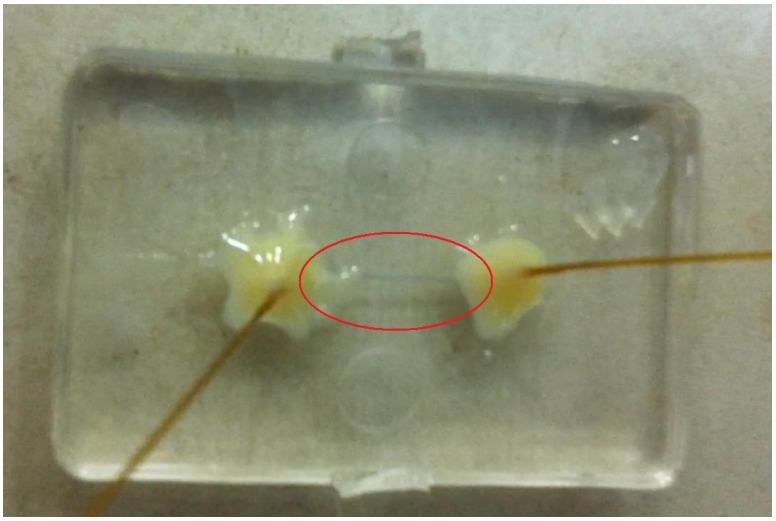

Figure 5.11: The microfluidic device loaded with blue ink

leakage. No leakage was observed within the microfluidic device. The microfluidic device loaded with blue ink can be seen in Figure 5.11.

Chapter 6

Summary and Future Research Directions

The ultimate goal of the microfluidics technology is to develop disposable devices which can accomplish biomedical analyses at much lower manufacturing and operational cost compared to its room-sized or benchtop-sized counter-parts. In this perspective, micro- and nano-scale fabrication of disposable medical devices is a popular topic both for research and commercial applications. Injection molding of structures with micro-features is a developing process with great potential for the mass-production of micro-scale devices with low-cost [1]. The major focus of this study is to develop a technique for repeatable, productive and accurate fabrication of microfluidic devices on a mass production scale. To achieve this, injection molding process is adapted for the fabrication of a microfluidic device which composed of a single microchannel.

A proper mold for the injection molding was designed and manufactured using high-precision mechanical machining. During the design procedure, numerical experimentation was performed using Moldflow® simulation tool. The microfluidic device was fabricated out of Plexiglass 6N. To analyze the effect of the mold temperature, both simulations and the injection molding of the microfluidic device were performed at different mold temperatures. The bonding of the microfluidic

device is performed by direct bonding and adhesive bonding. The practical aspects of two bonding techniques were assessed, and it was concluded that direct bonding more feasible than adhesive bonding. The warpage and the bonding quality of the final products were characterized for different mold temperatures. It was found that there exists one-to-one correspondence between the warpage and the bonding quality of the molded pieces. As the warpage of the pieces decresases, the bonding quality increases. A maximum point for the breaking pressure (which is the parameter used for the characterizatin of the bond quality) and the minimum point for the warpage was found which were observed at the same mold temperature. This mold temperature was named as the optimum mold temperature for a better quality. In this study, it was observed that although Moldflow® can be used as a design tool since it can predict many aspects of the molding process, Moldflow® cannot predict the optimum mold temperature. Moldflow® predicted an optimum mold temperature of 79°C, however, in the experiments it was found that the optimum mold temperature is around 45°C. For this optimum mold temperature, it is observed that a microfluidic device can withstand pressure up to 74 bars, which is very promising when HPLC applications are considered. Therefore, although Moldflow® is one of the powerful simulation tools for injection molding, it is better to use it for design check for the structures with micro-features instead of using for the optimization of the injection parameters. The ideal injection molding parameters depend on the injection molding machine, environmental conditions and complete mold geometry (not only mold cavity), which have considerably effects on the pieces with micro-featured parts compared to macro-sized parts.

The production of a single microfluidic device set (two piece) was performed nearly in fifteen seconds (depending on the mold temperature). However, the machining of the mold took approximately 4 hours. For the bonding of the microfluidic device another half an hour is required. However, considering the mold is manufactured for one time, and the bonding process can be automated, the fabrication of the polymeric microfluidic devices can be performed very fast with the injection method presented. Therefore, injection molding is a very promising method for the production of microfluidic device on a mass scale (about 10000

pieces/day with a single injection machine).

Although a microfluidic device with a single channel can be used in HPLC applications, generally in the biomedical application microfluidic devices with a rather complex microchannel network are needed. Since the framework of the fabrication of such a structure is similar to that of with a single microchannel, a similar research on a microfluidic device with a microchannel network will be an interesting future research direction. Moreover the limits of the fabrication can be extended and the investigation of injection molding of products with even sub-micron features can be one of the key research directions in this field. I believe that, as the field of injection of devices micro-features becomes more mature in terms of commercial applications, the overall manufacturing costs will continue to decrease which will increase the demand for micro-molding techniques.

Bibliography

[1] U. M. Attie, S. Marson, and J. R. Alcock, "Micro-injection moulding of polymer microfluidic devices," *Microfluid. Nanofluid.*, vol. 7, pp. 1–28, July 2009.

[2] N.-T. Nguyen, *Fabrication Technologies*, ch. 3, pp. 124–127. William Andrew, 2008.

[3] J. Giboz, T. Copponnex, and P. Mele, "Microinjection molding of thermoplastic polymers: A review," *J. Micromec. Microeng.*, vol. 17, pp. 96–109, 2007.

[4] R. H. Todd, *Manufacturing Processes Reference Guide*, p. 240. Industrial Press, 2004.

[5] I. Papautsky and E. T. K. Peterson, *Micromolding, Micro and Nanofluidic Encylopedia*, p. 1256. Springer, 2008.

[6] J. W. Hyatt, "First injection molding machine." American Patent Institue, #133229.

[7] History of Injection Molding. `http://www.avplastics.co.uk/a-short-history-of-injection-moulding`. Accessed: 2010-09-30.

[8] D. M. Bryce, *Plastic Injection Molding: Manufacturing Process Fundamentals*, pp. 1–2. Society of Manufacturing Engineering, 1996.

[9] H. Shin and E.-S. Park, "Analysis of incomplete filling defect for injection-molded air cleaner cover using moldflow simulation," *J. Poly.*, 2013.

[10] V. Shah, "Micro injection molding." http://www.consultekusa.com/pdf/Consulting/Process/MICRO\%20INJECTION\%20MOLDING.pdf. Accessed: 2013-10-20.

[11] P. K. Kennedy, *Practical and Scientific Aspects of Injection Molding Simulation*. PhD thesis, Melbourne University, 2008.

[12] G. Tosello and H. N. Hansen, "Micro injection molding," in *Micromanufacturing Engineering and Technology* (Y. Qin, ed.), ch. 6, pp. 1–2, William Andrew, 2010.

[13] J. D. Schieber, D. C. Venerus, K. Bush, V. Balasubramanian, and S. Smoukov, "Measurement of anisotropic energy transport in flowing polymers by using a holographic technique," *Proc. Nat. Acad. Sci.*, vol. 101, pp. 13142–13146, 2004.

[14] M. Heckele and W. K. Schomburg, "Review on micro molding of thermoplastic polymers," *J. Micromech. Microeng.*, vol. 14, 2003.

[15] V. Piotter, W. Bauer, T. Benzler, and A. Emde, "Injection molding of components for microsystems," *J. Microsyst. Technol.*, vol. 7, pp. 99–102, 2001.

[16] V. Piotter, K. Mueller, K. Plewa, R. Ruprecht, and J. Hausselt, "Performance and simulation of thermoplastic micro injection molding," *J. Microsyst. Technol.*, vol. 8, pp. 387–390, 2002.

[17] R. Bartolini, W. Hannan, D. Karlsons, and M. Lurie, "Embossed hologram motion pictures for television playback," *Appl. Opt.*, vol. 9, 1970.

[18] W. J. Hannan, R. E. Flory, and L. M. Ryan, "Holotape: A low-cost prerecorded television system using holographic storage," *J. Soc. Motion Pict. Telev. Eng.*, vol. 82, 1973.

[19] K. Knop, "Color pictures using the zero diffraction order of phase grating structures," *Opt. Commun.*, vol. 18, pp. 298–303, 1976.

[20] R. Ulrich, H. P. Weber, E. A. Chandross, W. J. Tomlinson, and E. A. Franke, "Embossed optical waveguides," *Appl. Phys. Lett.*, vol. 20, 1972.

[21] E. Becker, H. Betz, W. Ehrfeld, W. Glashauser, A. Heuberger, H. J. Michel, D. Munchmeyer, S. Pongartz, and R. V. Siemens, "Production of separation nozzle systems for uranium enrichment by a combination of X-ray lithography and galvanoplastics," *Naturwissenschaften*, vol. 69, 1982.

[22] W. Ehrfeld, P. Bley, F. Gotz, P. Hagmann, A. Maner, J. Mohr, H. O. Moser, D. Munchmeyer, W. Schelb, D. Schmidt, and E. W. Becker, *Fabrication of microstructures using the LIGA process.* IEEE Micro Robots and Teleoperators Workshop, 9–11 Nov. 1987.

[23] P. Hagmann, W. Ehrfeld, and H. Vollmer, *Fabrication of microstructures with extreme structural heights by reaction injection molding.* 1^{st} Meeting of the European Polymer Federation European Symp. on Polymeric Materials, 14–18 Sept. 1987.

[24] W. Menz, W. Bacher, M. Harmening, and A. Michel, *The LIGA technique novel concept for microstructures and the combination with Si-technologies by injection molding.* 4^{th} IEEE Workshop on MEMS, 31 Jan.–2 Feb. 1991.

[25] M. Harmening, W. Bacher, P.Bley, A. El-Kholi, H. Kalb, B. Kowanz, W. Menz, A. Michel, and J. Mohr, "Molding of three-dimensional microstructures by the liga process," *J. MEMS*, 1992.

[26] A. Michel, "Technique of application of mechanical microstructures onto microelectronic circuits," Master's thesis, Karlsruhe Univ., Germany, 1993.

[27] A. Both, W. Bacher, M. Heckele, K. D. Muller, R. Ruprecht, and M. Strohrmann, *Molding process with high alignment precision for the LIGA technology.* Proc. IEEE MEMS, Amsterdam, 29 Jan.–2 Feb. 1995.

[28] R. Ruprecht, H. Kalb, B. Kowanz, and W. Bacher, "Molding of liga microstructures from fluorinated polymers," *Microsyst. Technol.*, vol. 2, 1996.

[29] M. Heckele, "Aufbau und betrieb einer kleinserienfertigung von liga-spektrometern," *Swiss Plastics*, vol. 19, 1997.

[30] L. Baraldi, R. E. Kunz, and J. Meissner, "High-precision molding of integrated optical structures," *Proc. SPIE*, 1993.

[31] M. T. Gale, L. G. Baraldi, and R. E. Kunz, "Replicated microstructures for integrated optics," *Proc. SPIE*, 1994.

[32] M. Gerner, T. Paatzsch, L. Weber, H. Schift, I. Smaglinski, H. D. Bauer, M. Abraham, and W. Ehrfeld, *Micro-optical components for fiber and integrated optics realized by the LIGA technique.* Proc. MEMS, IEEE, Amsterdam, 29 Jan.–2 Feb. 1995.

[33] K. Haines, "Development of embossed holograms," *Proc. SPIE*, vol. 2652, pp. 45–52, 1996.

[34] T. G. Harvey, "Replication techniques for micro-optics," *Proc. SPIE*, vol. 3099, pp. 76–82, 1997.

[35] S. Kalveram and A. Neyer, "Precision molding techniques for optical waveguide devices," *Proc. SPIE*, vol. 3125, pp. 2–11, 1997.

[36] A. Olsson, O. Larsson, J. Holm, L. Lundbladh, O. Ohman, and G. Stemme, *Valve-less diffuser micropumps fabricated using thermoplastic replication.* Proc. IEEE 10^th Annu. Int. Workshop on MEMS, 26 Jan.–30 Jan. 1997.

[37] L. Lin, Y. T. Cheng, and C. J. Chiu, "Comparative study of hot embossed micro structures fabricated by laboratory and commercial environments," *Microsyst. Technol.*, vol. 4, 1998.

[38] R. M. McCormick, R. J. Nelson, M. G. Alonso-Amigo, D. J. Benvegnu, and H. Hooper, "Microchannel electrophoretic separations of dna in injection-molded plastic substrates," *Anal. Chem.*, vol. 69, 1997.

[39] L. Martynova, L. E. Locascio, M. Gaitan, G. W. Kramer, R. G. Christensen, and W. A. MacCrehan, "Fabrication of plastic microfluid channels by imprinting methods," *Anal. Chem.*, vol. 69, no. 12, 1997.

[40] H. Becker and W. Dietz, "Microfluidic devices for μ-TAS applications fabricated by polymer hot embossing," *Proc. SPIE*, vol. 3515, 1998.

[41] B. Bustgens, W. Bacher, W. Bier, R. Ehnes, D. Maas, R. Ruprecht, W. K. Schomburg, and L. Keydel, *Micromembrane pump manufactured by molding Actuator.* Proc. 4^{th} Int. Conf. on New Actuators, Bremen, 1994.

[42] L. Weber and W. Ehrfeld, *Molding of Microstructures for High-tech Applications*. 56^{th} Annual Technical Conference (ANTEC), Atlanta, GA, USA, 30 April 1998.

[43] M. Niggemann, W. Ehrfeld, and L. Weber, *Fabrication of Miniaturized Biotechnical Devices*. The International Society for Optical Engineering, Santa Clara, CA, 21–22 September 1998.

[44] A. Angelov and I. Coulter, *Micromolding Product Manufacture–A Progress Report*. Annual Technical Conference (ANTEC), Chicago,IL, USA, 16–20 May 2004.

[45] L. Weber, W. Ehrfeld, H. Freimuth, M. Lacher, H. Lehr, and B. Pech, *Micromolding: A Powerful Tool for Large-scale Production of Precise Microstructures*. International Society for Optical Engineering, Austin, TX, USA, 14–15 October 1996.

[46] L. Weber and W. Ehrfeld, "Micro-moulding–processes, moulds, applications," *Kunsts Plast. Eur.*, pp. 3–60, 1998.

[47] R. Ruprecht, T. Hanemann, V. Piotter, and J. HauBelt, "Polymer materials for microsystem technologies," *Microsyst. Technol.*, pp. 44–48, 1998.

[48] W. K. Schomburg, R. Ahrens, W. Bacher, J. Martin, and V. Saile, "Amanda surface micromachining, molding, and diaphragm transfer," *Sens. Actuators*, vol. 76, 1999.

[49] L. Malaquin, F. Carcenac, C. Vieu, and M. Mauzac, "Using polydimethylsiloxane as a thermocurable resist for a soft imprint lithography process," *Microelectron. Eng.*, vol. 61–62, 2002.

[50] J. Dopper, M. Clemens, W. Ehrfeld, K. P. Kamper, and H. Lehr, "Development of low-cost injection molded micropumps," in *Proc. Actuators*, June 26–28 1996.

[51] J. Fahrenberg, W. Bier, D. Maas, W. Menz, R. Ruprecht, and W. K. Schomburg, "Microvalve system fabricated by thermoplastic molding," *J. Micromech. Microeng.*, vol. 5, pp. 71–169, 1995.

[52] C. Goll, W. Bacher, B. Butgens, D. Maas, R. Ruprecht, and W. K. Schomburg, "Electrostatically actuated polymer microvalve equipped with a movable membrane electrode," *J. Micromech. Microeng.*, vol. 7, pp. 6–224, 1997.

[53] J. Martin, W. Bacher, O. F. Hagena, and W. K. Schomburg, *Strain gauge pressure and volume-flow transducers made by thermoplastic molding and membrane transfer.* Proc. Int. Workshop on MEMS, Heidelberg, Germany, 25–29 Jan. 1998.

[54] M. J. Madou, *Fundamentals of Microfabrication: The Science of Miniaturization*, p. 752. CRC Press (2^{nd} ed.), 2002.

[55] F. Group, "Injection molded plastics technical report," 2004.

[56] H. Becker, "Microfluidics: A technology coming of age," *Medical Device Technology*, pp. 21–24, 2008.

[57] V. Piotter, A. Guber, M. Heckele, and A. Gerlach, *Micro Moulding of Medical Device Components.* Business Briefing: Medical Device Manufacturing & Technology, 2004.

[58] H. Becker and C. Gartner, "Polymer microfabrication methods for microfluidic analytical applications," *Electrophoresis*, 2000.

[59] V. Piotter, T. Hanemann, R. Ruprecht, and J. HauBelt, *Micro-injection Molding of Medical Device Components.* Business Briefing: Medical Device Manufacturing & Technology, 2002.

[60] Bartels Microtechnik. `http://www.bartels-mikrotechnik.de`. Accessed: 2013-10-20.

[61] ThinXXS. `http://www.thinxxs.com/`. Accessed: 2013-09-30.

[62] Micralyne. `http://www.micralyne.com/`. Accessed: 2013-09-30.

[63] Microfluidic ChipShop. `http://www.microfluidic-chipshop.com/`. Accessed: 2013-09-30.

[64] J. Catanzaro and B. Kadykowski, *Micro Molding–A New Way.* Annual Technical Conference (ANTEC), 2002.

[65] T. Shepard and D. Dunn, *Micro-injection Molding of Medical Products: Machine Specification and Process Simulation.* Annual Technical Conference (ANTEC), 1995.

[66] T. Hanemann, M. Heckele, and V. Piotter, "Current status of micromolding technology," *Polym. News*, vol. 25, pp. 9–224, 2000.

[67] M. G. Robinson and J. M. Jackson, *Etching, Machining, and Molding High-Aspect Ratio Microstructures*, ch. 3, pp. 59–85. CRC Press, 2005.

[68] Mitsubishi Engineering-Plastics Corporation. `http://www.m-ep.co.jp/en/pdf/product/reny/mold_designing.pdf`. Accessed: 2013-09-30.

[69] ToolingU-SME. `http://www.toolingu.com/definition-500255-54082-mold-unit.html`. Accessed: 2013-09-30.

[70] N. Gottschlich, "Production of plastic components for microfluidic applications." `http://www.touchbriefings.com/pdf/855/fdd041_greiner_tech.pdf`, 2004. Accessed: 2010-10-20.

[71] T. Boone, Z. HughFan, H. Hooper, A. Ricco, H. Tan, and S. Williams, "Plastic advances microfluidic devices," *Anal. Chem.*, vol. 74, p. 3, 2002.

[72] L. Yu, C. Koh, L. Lee, K. Koelling, and M. Madou, "Experimental investigation and numerical simulation of injection molding with micro-features.," *Polym. Eng. Sci.*, vol. 42(5), pp. 871–888, 2002.

[73] G. Xu, D. Kim, K. Koelling, and L. Lee, "Flow dynamics in injection molding with microfeatures.," in *Proc. the Annual Technical Conference, (ANTEC)*, (Boston, MA.), 2005.

[74] A. D. Mello, "Plastic fantastic," *Lab Chip Minituarisation Chem. Biol.*, vol. 2(2), 2002.

[75] City University of Hong Kong. `www.cityu.edu.hk/meem/seminar/24_april_2_2001.html`. Accessed: 2010-09-30.

[76] C. Hieber and S. Shen, "A finite element / finite difference simulation of the injection molding filling process.," *J. Non-Newtonian Fluid Mech.*, vol. 7, pp. 1–32, 1980.

[77] CoreTech System Co. Ltd. http://www.moldex3d.com/en/. Accessed: 2013-09-30.

[78] Autodesk–Moldflow. http://www.autodesk.com/products/autodesk-simulation-family/features/simulation-moldflow. Accessed: 2013-09-30.

[79] SIGMA Engineering GmbH. http://www.sigmasoft.de/ftp/web/module_thermal_en/index.php. Accessed: 2013-09-30.

[80] Epicor. http://www.epicor.com/Industries/Manufacturing/Pages/Rubber.aspx. Accessed: 2013-09-30.

[81] ProMax-One^{TM} InjecNet. http://injecnet.com/. Accessed: 2013-09-30.

[82] P. Nguyen, X. Chen, C. Lam, and Y. Yue, "Effects of polymer melt compressibility on mold filling in micro-injection molding," *J. Micromech. Microeng.*, vol. 21, no. 9, 2011.

[83] Autodesk, "Moldflow advisor," *User Manual*, 2012.

[84] Engineering Design Center. http://www.dc.engr.scu.edu/cmdoc/dg_doc/develop/process/physics/b3500001.htm. Accessed: 2013-09-30.

[85] C. Ahn, J. Choi, G. Beaucage, J. Nevin, J. Lee, Puntambekar, and J. Lee, "Disposable smart lab on a chip for point of care clinical diagnostics," in *Proc. the IEEE*, vol. 92, pp. 154–173, 2004.

[86] W. Wang and S. A. Soper, *BioMEMS: Technologies and Applications*. CRC Press, 2007.

[87] H. Becker and U. Heim, "Hot embossing as amethod for the fabrication of polymer high aspect ratio structures," *Sens. Actuators*, vol. 83, pp. 130–135, 2000.

[88] Güvenal Hırdavat. `http://www.guvenal.net/`. Accessed: 2013-09-30.

[89] M. Stjernstrom and J. Roeraade, "Method for fabrication of microfluidic system in glass," *J. Micromech. Microeng.*, vol. 8, pp. 33–38, 1998.

[90] W. Ko, "Bonding techniques for microsensors," *J. Micromachining and Micropackaging of Transducers*, pp. 41–61, 1985.

[91] M. Weckwerth, "Epoxy bond and stop-etch EBASE technique enabling backside processing of Al GaAs heterostructures," *Superlattices Microstructures*, vol. 20, pp. 561–567, 1996.

[92] H. Nguyen, "A substrate-independent wafer transfer technique for surface micromachined devices," in *13th IEEE International Workshop MEMS*, (Miyazaci, Japan), pp. 628–632, 2000.

Appendix A

TECHNICAL DRAWING OF THE MOLD

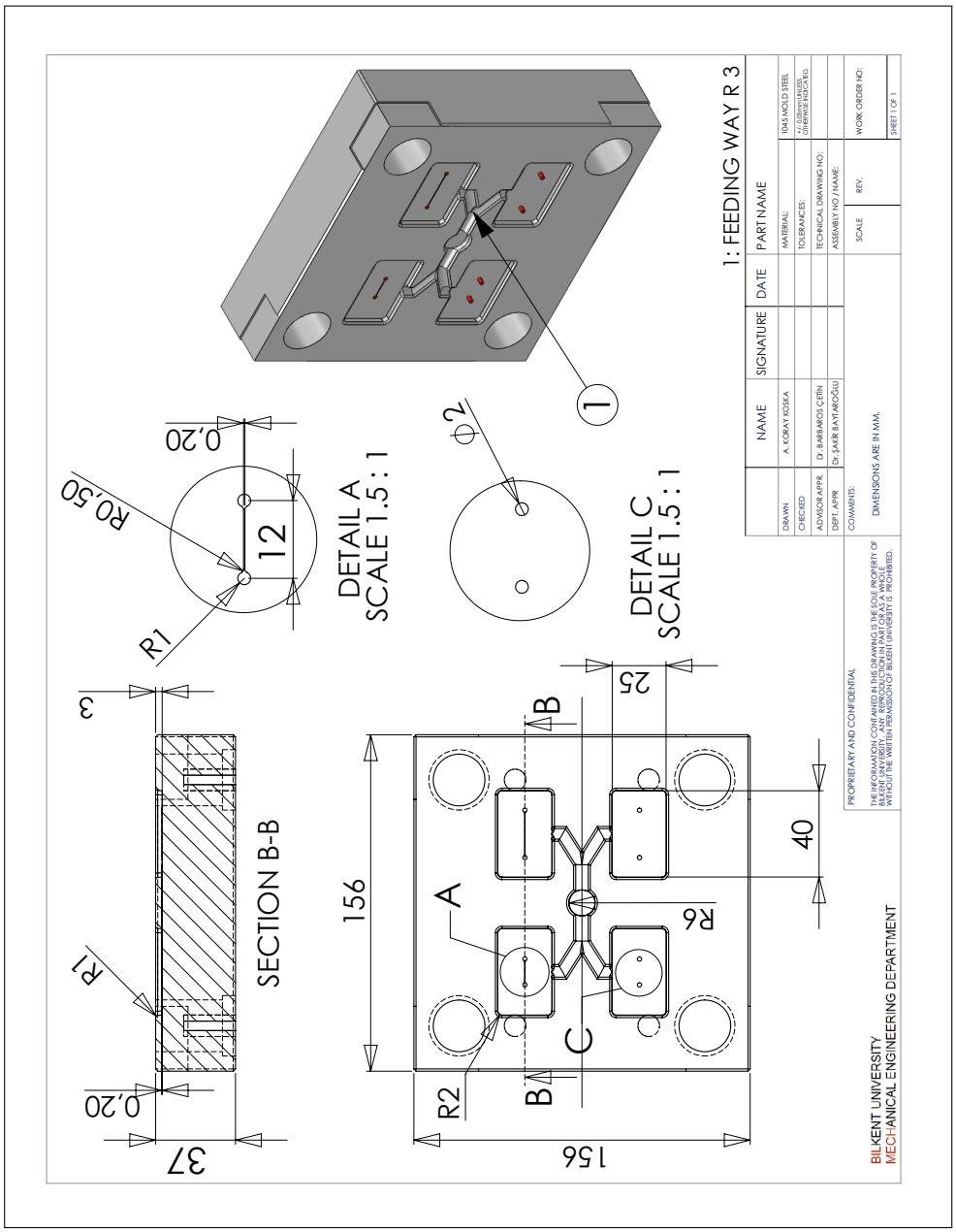

Figure A.1: Technical drawing of the mold

Appendix B

MATERIAL DATA SHEET

PLEXIGLAS®

Product Information

PLEXIGLAS® 6N

Product Profile:

PLEXIGLAS® 6N is an amorphous thermoplastic molding compound (PMMA).

Typical properties of PLEXIGLAS® molding compounds are:
- good flow
- high mechanical strength, surface hardness and mar resistance
- high light transmission
- excellent weather resistance
- free colorability due to crystal clarity.

The special properties of PLEXIGLAS® 6N are:
- very good mechanical properties
- high heat deflection temperature
- excellent flow / melt viscosity

Application:

Particularly suitable for injection molding optical and technical items.

Examples:

optical waveguides, luminaire covers, automotive lighting, instrument cluster covers, optical lenses, displays, cuvettes, medical applications etc.

Processing:

PLEXIGLAS® 6N can be processed on injection molding machines with 3-zone general purpose screws for engineering thermoplastics.

Physical Form / Packaging:

PLEXIGLAS® molding compounds are supplied as pellets of uniform size, packaged in 25kg polyethylene bags or in 500kg boxes with PE lining; other packaging on request.

For more information:

For more information, e.g. Charts or lists of resistance are in the database CAMPUS ® (http://www.campusplastics.com) free of charge.

Figure B.1: Material data sheet (p.1)

Properties:

	Parameter	Unit	Standard	PLEXIGLAS® 6N
Mechanical Properties				
Tensile Modulus	1 mm/min	MPa	ISO 527	3200
Stress @ Break	5 mm/min	MPa	ISO 527	67
Strain @ Break	5 mm/min	%	ISO 527	3
Charpy Impact Strength	23°C	kJ/m²	ISO 179/1eU	20
Thermal Properties				
Vicat Softening Temperature	B / 50	°C	ISO 306	96
Coeff. of Linear Therm. Expansion	0 - 50°C	E-5 /°K	ISO 11359	8
Fire Rating			DIN 4102	B2
Flammability UL 94	1.6 mm	Class	IEC 707	HB
Rheological Properties				
Melt Volume Rate, MVR	230°C / 3.8kg	cm³/10min	ISO 1133	12
Optical Properties	d=3 mm			
Luminous transmittance	D65	%	ISO 13468-2	92
Refractive Index			ISO 489	1.49
Other Properties				
Density		g/cm³	ISO 1183	1.19
Recommended Processing Conditions				
Predrying Temperature		°C		max. 85
Predrying Time in Desiccant-Type Drier		h		2 - 3
Melt Temperature		°C		220 - 260
Mold Temperature (Injection Molding)		°C		60 - 90

All listed technical data are typical values intended for your guidance. They are given without obligation and do not constitute a materials specification.

Evonik Industries AG Kirschenallee 64293 Darmstadt
Telefon +49 6151 18-4711 Telefax +49 6151 18-3177
www.plexiglas-polymers.com

Ref. No.: MC104-E V0160 Date: 2013-02-05

Evonik. Power to create.

EVONIK INDUSTRIES

Figure B.2: Material data sheet (p.2)

Appendix C

WARPAGE MEASUREMENT RESULTS

VK-X100 3D laser microscope measurement results are listed below for each mold temperatures. Selected bonding area, horizontal distance, height difference and calculated part deformation are given in the tables.

C.1 Measurement in the $x-$up direction for different mold temperatures

Measurements of the $x-$up direction are listed from table D.1 to table D.6. Measured area can be seen in Figure D.1.

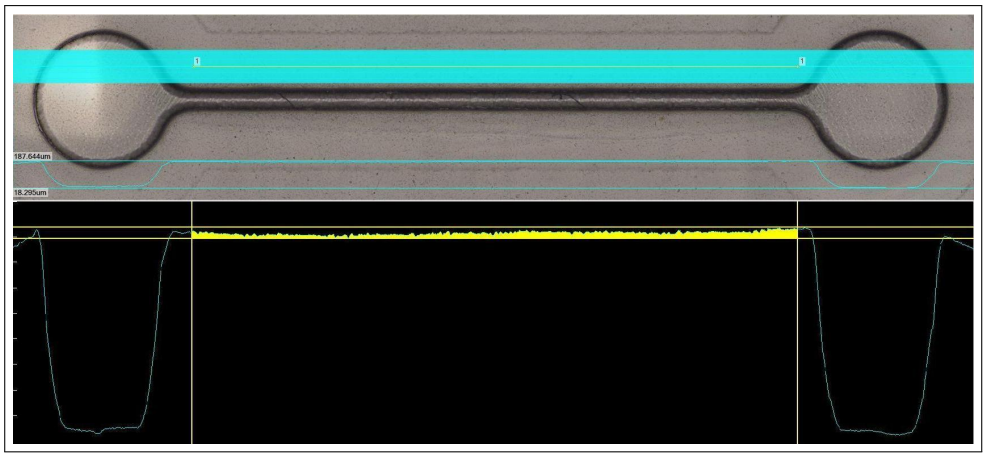

Figure C.1: Measured area (x-up)

Table C.1: Measurements of the samples at a mold temperature of 35°C

# of Samples	Area [μm^2]	Horizontal Distance [μm]	Height Difference [μm]	Deformation [μm]
Sample 1	101503	9074.54	20.455	9.270
Sample 2	91864.6	9159.31	19.102	9.072
Sample 3	44513.4	9565.15	12.673	8.019
Sample 4	56508.8	9419.58	13.708	7.709
Sample 5	40557.8	9268.88	12.906	8.530
Sample 6	44239.6	9551.31	13.08	8.448

Table C.2: Measurements of the samples at a mold temperature of 45°C

# of Samples	Area [μm^2]	Horizontal Distance [μm]	Height Difference [μm]	Deformation [μm]
Sample 1	46385.2	9030.91	9.764	4.628
Sample 2	41143.8	9291.99	9.407	4.979
Sample 3	35398.6	9271.44	6.379	2.561
Sample 4	54590.8	9508.52	10.778	5.037
Sample 5	39688.7	9311.68	8.99	4.728
Sample 6	40427.7	9310.51	8.894	4.552

Table C.3: Measurements of the samples at a mold temperature of 55°C

# of Samples	Area [μm^2]	Horizontal Distance [μm]	Height Difference [μm]	Deformation [μm]
Sample 1	48965.4	8905.78	18.927	13.429
Sample 2	48922.7	8929.01	22.018	16.539
Sample 3	104455	9590.84	23.974	13.083
Sample 4	57348	9499.96	17.432	11.395
Sample 5	55966.3	9414.38	19.57	13.625
Sample 6	43304.5	9405.82	17.275	12.671

Table C.4: Measurements of the samples at a mold temperature of 65°C

# of Samples	Area [μm^2]	Horizontal Distance [μm]	Height Difference [μm]	Deformation [μm]
Sample 1	56652.5	9207.08	23.897	17.744
Sample 2	151358	9747.67	33.623	18.095
Sample 3	76954.5	9456.44	28.228	20.090
Sample 4	76912.2	9308.25	31.57	23.307
Sample 5	97731.4	9399.85	33.011	22.614
Sample 6	62892.9	9673.8	24.345	17.844

Table C.5: Measurements of the samples at a mold temperature of 75°C

# of Samples	Area [μm^2]	Horizontal Distance [μm]	Height Difference [μm]	Deformation [μm]
Sample 1	176297	9607.97	44.348	25.999
Sample 2	83191.7	9750.85	41.71	33.178
Sample 3	117925	9635.71	46.52	34.282
Sample 4	100395	9573.71	38.245	27.758
Sample 5	97991.1	9605.32	37.883	27.681
Sample 6	140849	9705.37	41.172	26.660

Table C.6: Measurements of the samples at a mold temperature of 85°C

# of Samples	Area [μm^2]	Horizontal Distance [μm]	Height Difference [μm]	Deformation [μm]
Sample 1	280794	9642.22	66.14	37.019
Sample 2	218004	9767.97	48.998	26.680
Sample 3	240112	9436.7	70.309	44.865
Sample 4	232396	9633.66	55.199	31.076
Sample 5	319590	9582.28	66.562	33.210
Sample 6	280754	9553.95	63.128	33.742

C.2 Measurement in the $x-$bottom direction for different mold temperatures

Measurements of the $x-$bottom direction are listed from table D.7 to table D.12. Measured area can be seen in Figure D.2.

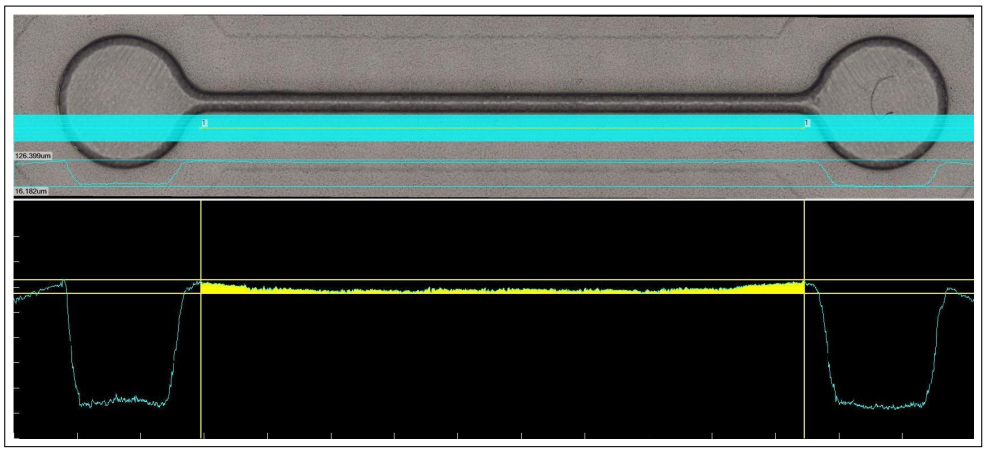

Figure C.2: Measured area (x-bottom)

Table C.7: Measurements of the samples at a mold temperature of 35°C

# of Samples	Area [μm^2]	Horizontal Distance [μm]	Height Difference [μm]	Deformation [μm]
Sample 1	61273.9	9517.08	11.879	5.441
Sample 2	35995.1	9507.83	10.785	6.999
Sample 3	60836.2	9690.93	12.027	5.749
Sample 4	59461.2	9548.68	13.855	7.628
Sample 5	35414.8	9696.81	9.675	6.023
Sample 6	57484.7	9474.29	13.663	7.596

Table C.8: Measurements of the samples at a mold temperature of 45°C

# of Samples	Area [μm^2]	Horizontal Distance [μm]	Height Difference [μm]	Deformation [μm]
Sample 1	27484.8	9259.43	8.902	5.934
Sample 2	40945.1	9420.34	9.96	5.614
Sample 3	34367.4	9297.12	6.567	2.870
Sample 4	44626.1	9371.59	10.778	6.016
Sample 5	34761	9054.92	7.764	3.925
Sample 6	55380.6	9302.62	11.155	5.202

Table C.9: Measurements of the samples at a mold temperature of 55°C

# of Samples	Area [μm^2]	Horizontal Distance [μm]	Height Difference [μm]	Deformation [μm]
Sample 1	62155.7	9399.85	19.99	13.378
Sample 2	43768.3	9502.59	21.393	16.787
Sample 3	98517.4	9462.39	21.741	11.330
Sample 4	64616.1	9328.79	17.994	11.067
Sample 5	48582.1	9226.09	17.204	11.938
Sample 6	47904.3	9559.87	18.454	13.433

Table C.10: Measurements of the samples at a mold temperature of 65°C

# of Samples	Area [μm^2]	Horizontal Distance [μm]	Height Difference [μm]	Deformation [μm]
Sample 1	51778.9	9267.09	21.786	16.199
Sample 2	113822	9773.36	29.062	17.416
Sample 3	78379.5	9310.82	28.228	19.810
Sample 4	94077	9333.94	30.113	20.034
Sample 5	81485	9648.12	28.885	20.439
Sample 6	63928.4	9511.15	25.899	19.178

Table C.11: Measurements of the samples at a mold temperature of 75°C

# of Samples	Area [μm^2]	Horizontal Distance [μm]	Height Difference [μm]	Deformation [μm]
Sample 1	465223	9667.91	68.332	20.212
Sample 2	104199	9870.7	34.942	24.386
Sample 3	161256	9489.98	48.426	31.434
Sample 4	84845.2	9685.04	32.597	23.837
Sample 5	115230	9793.66	36.184	24.418
Sample 6	140857	9739.6	36.805	26.660

Table C.12: Measurements of the samples at a mold temperature of 85°C

# of Samples	Area [μm^2]	Horizontal Distance [μm]	Height Difference [μm]	Deformation [μm]
Sample 1	427742	9599.4	81.521	36.962
Sample 2	212656	9716.61	49.315	27.429
Sample 3	117377	9847.74	45.591	33.672
Sample 4	191333	9847.74	46.096	26.667
Sample 5	162124	9813.48	48.123	31.602
Sample 6	176427	9365.61	71.586	52.748

C.3 Measurement in $y-$up direction for different mold temperatures

Measurements of the $y-$up direction are listed from table D.13 to table D.18. Measured area can be seen in Figure D.3.

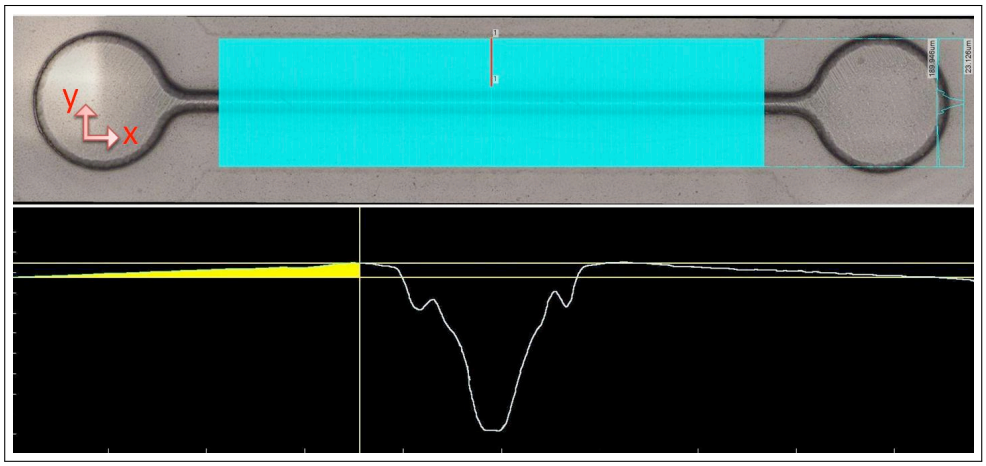

Figure C.3: Measured area (y-up)

Table C.13: Measurements of the samples at a mold temperature of 35°C

# of Samples	Area [μm^2]	Horizontal Distance [μm]	Height Difference [μm]	Deformation [μm]
Sample 1	4948.04	710.573	13.975	7.012
Sample 2	2413.92	713.332	10.24	6.856
Sample 3	3004.68	794.703	14.138	10.357
Sample 4	7227.98	784.937	16.034	6.826
Sample 5	1589.3	788.906	10.615	8.600
Sample 6	2253.06	801.247	16.077	13.265

Table C.14: Measurements of the samples at a mold temperature of 45°C

# of Samples	Area [μm^2]	Horizontal Distance [μm]	Height Difference [μm]	Deformation [μm]
Sample 1	1645.81	770.197	8.495	6.358
Sample 2	3023.26	713.904	9.701	5.466
Sample 3	2294.7	732.4	5.863	2.730
Sample 4	5195.76	734.543	12.923	5.850
Sample 5	5407.21	797.793	11.589	4.811
Sample 6	3557.06	730.076	11.589	6.542

Table C.15: Measurements of the samples at a mold temperature of 55°C

# of Samples	Area [μm^2]	Horizontal Distance [μm]	Height Difference [μm]	Deformation [μm]
Sample 1	8263.03	796.598	21.602	11.229
Sample 2	6783.46	728.054	20.359	11.042
Sample 3	2862.3	781.727	18.895	15.233
Sample 4	4430.64	804.518	22.802	17.295
Sample 5	5478.65	777.362	23.202	16.154
Sample 6	7488.13	725.311	23.602	13.278

Table C.16: Measurements of the samples at a mold temperature of 65°C

# of Samples	Area [μm^2]	Horizontal Distance [μm]	Height Difference [μm]	Deformation [μm]
Sample 1	2938.96	778.493	24.402	20.627
Sample 2	5709.36	786.414	31.203	23.943
Sample 3	6284.42	707.207	29.603	20.717
Sample 4	5612.65	769.441	28.002	20.708
Sample 5	5665.89	792.071	29.603	22.450
Sample 6	5520.3	795.466	26.002	19.062

Table C.17: Measurements of the samples at a mold temperature of 75°C

# of Samples	Area [μm^2]	Horizontal Distance [μm]	Height Difference [μm]	Deformation [μm]
Sample 1	10009.9	779.625	48.004	35.165
Sample 2	5574.89	783.019	36.003	28.883
Sample 3	5601.63	789.808	39.203	32.111
Sample 4	5273.98	761.52	38.403	31.477
Sample 5	5126.76	779.625	34.403	27.827
Sample 6	5439.48	788.677	39.604	32.707

Table C.18: Measurements of the samples at a mold temperature of 85°C

# of Samples	Area [μm^2]	Horizontal Distance [μm]	Height Difference [μm]	Deformation [μm]
Sample 1	7695.26	791.486	43.779	34.056
Sample 2	4418.87	789.161	52.02	46.421
Sample 3	4385.14	787.999	48.929	43.364
Sample 4	4586.15	790.323	53.565	47.762
Sample 5	4663.64	796.135	55.626	49.768
Sample 6	4500.12	797.297	51.505	45.861

C.4 Measurement in the $y-$bottom direction for different mold temperatures

Measurements of the $y-$bottom direction are listed from table D.19 to table D.24. Measured area can be seen in Figure D.4.

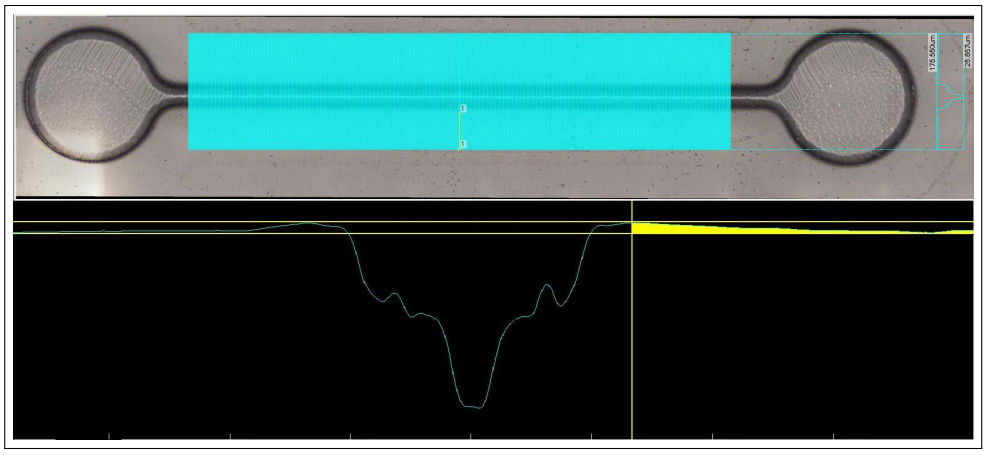

Figure C.4: Measured area (y-bottom)

Table C.19: Measurements of the samples at a mold temperature of 35°C

# of Samples	Area [μm^2]	Horizontal Distance [μm]	Height Difference [μm]	Deformation [μm]
Sample 1	4956.93	685.382	15.066	7.834
Sample 2	6616.96	746.102	18.222	9.353
Sample 3	2972.01	705.688	16.494	12.282
Sample 4	7073.51	755.088	18.325	8.957
Sample 5	6032.66	720.565	16.77	8.398
Sample 6	3000.19	753.018	12.94	8.956

Table C.20: Measurements of the samples at a mold temperature of 45°C

# of Samples	Area [μm^2]	Horizontal Distance [μm]	Height Difference [μm]	Deformation [μm]
Sample 1	2664.25	685.098	8.495	4.606
Sample 2	4526.98	746.102	12.254	6.186
Sample 3	2461.09	672.635	7.957	4.298
Sample 4	2725.92	630.671	9.387	5.065
Sample 5	2348.66	568.298	9.588	5.455
Sample 6	3791.07	756.307	10.615	5.602

Table C.21: Measurements of the samples at a mold temperature of 55°C

# of Samples	Area [μm^2]	Horizontal Distance [μm]	Height Difference [μm]	Deformation [μm]
Sample 1	5477.86	785.282	22.402	15.426
Sample 2	5422.76	785.282	18.802	11.897
Sample 3	4202.5	782.774	18.895	13.526
Sample 4	3103.07	792.071	22.002	18.084
Sample 5	7451.45	701.549	25.602	14.981
Sample 6	4040.26	785.282	21.202	16.057

Table C.22: Measurements of the samples at a mold temperature of 65°C

# of Samples	Area [μm^2]	Horizontal Distance [μm]	Height Difference [μm]	Deformation [μm]
Sample 1	4727.94	756.994	26.802	20.556
Sample 2	7289.26	771.704	28.803	19.357
Sample 3	7289.26	779.625	33.603	24.253
Sample 4	2314.57	759.257	22.802	19.754
Sample 5	2365.68	767.178	26.402	23.318
Sample 6	9854.45	769.441	34.403	21.596

Table C.23: Measurements of the samples at a mold temperature of 75°C

# of Samples	Area [μm^2]	Horizontal Distance [μm]	Height Difference [μm]	Deformation [μm]
Sample 1	6677.03	758.126	37.203	28.396
Sample 2	6539.45	764.915	33.603	25.054
Sample 3	7193.78	787.545	36.003	26.869
Sample 4	8450.71	769.441	40.004	29.021
Sample 5	8418.04	778.493	34.403	23.590
Sample 6	8450.71	783.019	41.604	30.812

Table C.24: Measurements of the samples at a mold temperature of 85°C

# of Samples	Area [μm^2]	Horizontal Distance [μm]	Height Difference [μm]	Deformation [μm]
Sample 1	6086.71	748.483	47.899	39.767
Sample 2	6910.62	721.751	42.749	33.174
Sample 3	10751.1	746.158	48.414	34.005
Sample 4	11960.9	774.052	50.99	35.538
Sample 5	8635.57	790.323	44.809	33.882
Sample 6	8761.32	764.754	49.444	37.988